Improvement in the Accuracy of PET Signals by Analysis of Textural Heterogeneity Parameters

Dissertation

zur Erlangung des Doktorgrades (MD/PhD)

der Medizinischen Fakultät

der Rheinischen Friedrich-Wilhelms-Universität

Bonn

Zain Khurshid

aus

Islamabad, Pakistan

2018

Angefertigt mit der Genehmigung

der Medizinischen Fakultät der Universität Bonn

1. Gutachter: Prof. Dr. med. Markus Essler

2. Gutachter: Prof. Dr.med. Alexander Drzezga

Tag der Mündlichen Prüfung: 26.09.2018

Aus der Klinik und Poliklinik für Nuklearmedizin

Direktor: Prof. Dr. med. Markus Essler

Index

1. Introduction

1.1 Assessment of tumor textural heterogeneity in PET scans

Since last three decades PET (positron emission tomography) is serving as the work horse in the diagnosis and management of oncological disorders. Since its introduction as a highly effective functional imaging technique PET has continually played its role in various aspects for example confirmation of diagnosis, tumor staging and re-staging, tumor efficacy assessment both during and after treatment and radiotherapy planning (Gallamini et al., 2014). Overtime there has been a continuous progress in the enhancement of PET use with the introduction of new radionuclides for imaging and software developments. One of such important technological development is the application of tumor textural heterogeneity in PET images.

Different imaging modalities for example X-rays, ultrasonography, computerized tomography (CT), magnetic resonance imaging (MRI) and PET are applied for the assessment of appearance and spread of the lesions. These modalities can be used depending on the tumor type and the location of lesions. The interpretation of all these modalities is essentially visual. However, there are features within each image that cannot be apprehended by the naked eye. Furthermore, when images are analyzed in a more quantitative manner, standard region of interest analysis may provide a mean parameter value, e.g., Hounsfield unit (HU) on CT, signal intensity (SI) on MRI, or standardized uptake value (SUV) on PET, but does not typically describe the underlying spatial distribution (Davnall et al., 2012).

Tumors are heterogeneous both on genetic and histopathological levels. Despite the fact that tumors usually originate from a single cell, human cancers frequently display substantial intra-tumor heterogeneity in virtually all distinguishable phenotypic features,

such as cellular morphology, gene expression (including the expression of cell surface markers and growth factor and hormonal receptors), metabolism, motility, and angiogenic, proliferative, immunogenic, and metastatic potential (Fidler and Hart, 1982; Dick, 2008; Nicolson, 1984; Heppner, 1984). A large number of cell divisions is required for genetic instability and thus highly malignant cell lines. It can be believed that there is presence of very diverse tumor cell clones in a tumor. The existence of tumoral heterogeneity at clonal level has been observed and documented for a variety of malignancies, including leukemias, breast, prostate, colon, brain, esophagus, head and neck, bladder, and gynecological carcinomas. This genetic heterogeneity translates into phenotypic heterogeneity evident as spatial variation with in the tumor. Tumors with high intratumoral heterogeneity have been shown to have poorer prognosis, which could be secondary to intrinsic aggressive biology or treatment resistance (Hockel et al., 1993, 1996; Yang et al., 2011). Figure 1 shows some of the precursors for high tumoral heterogeneity.

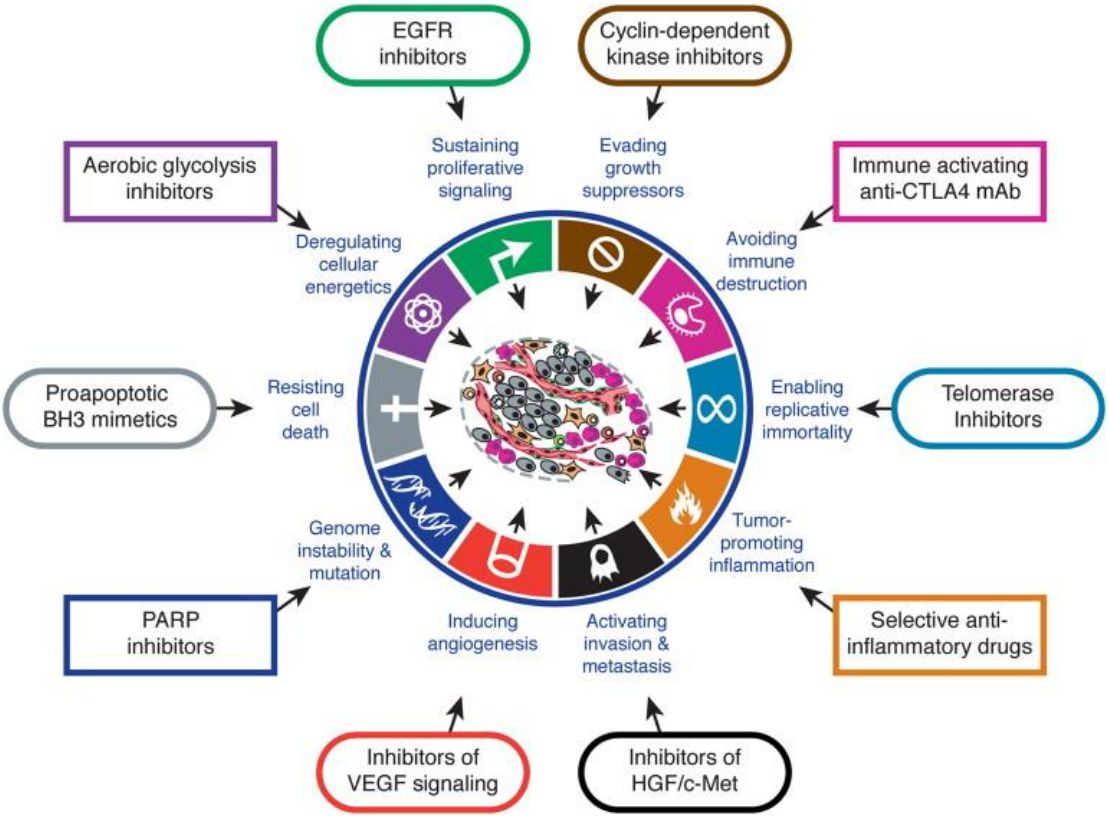

ill 1: Genetic precursors of high genetic heterogeneity (Hanahan D, Weinberg RA, 2011)

The identification of tumor heterogeneity in a tumor can be helpful in effective lesion characterization and therapy planning. It is not possible to assess intratumoral heterogeneity with biopsy as biopsy is a probe into a very small area of tumor and cannot inform about the full extent of phenotypic and genetic variation within the tumor (Gerlinger et al., 2012). Therefore, a non-invasive imaging method for assessing the tumor heterogeneity is of utmost importance as this can help in selecting patients with poor prognosis and an attempt can be made in redesigning the treatment which is vital part of personalized therapy. Numerous studies with good outcomes have shown that measurement of tumor textural heterogeneity by PET can a quantifiable parameter and can be easily applied.

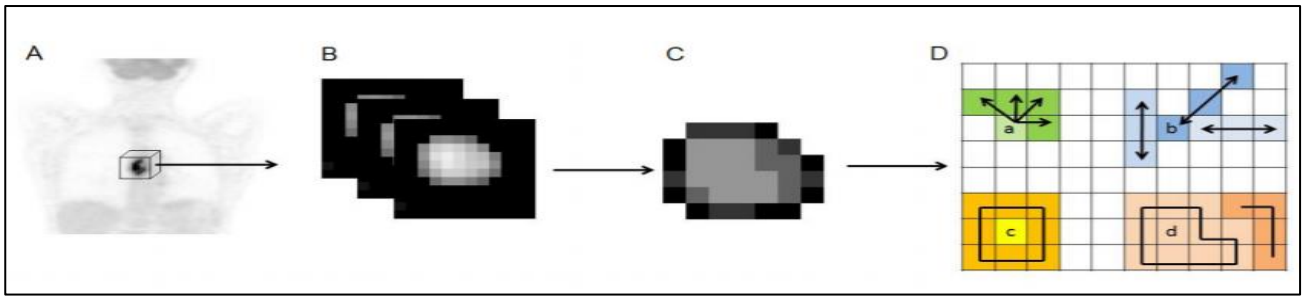

ill 2: Assessment of textural heterogeneity (A). Whole-body ^{18}F-FDG PET scan (B). Tumor segmentation (C). Voxel intensity resampling allowing (D). The extraction of different features (Tixier et al., 2011)

1.2 Texture Analysis

Texture analysis refers to a variety of mathematical methods that can be used to evaluate the intensity level and position of the pixels within an image, or a part of image, to derive so-called 'texture features' that provide a measure of intralesional heterogeneity (Castellano et al., 2004). Different methods have been applied, including statistical-, model-, and transform-based methods (Al-Kadi and Watson, 2008; Ganeshan et al., 2007; brown and Frayne, 2008; Gog et al., 2009; Sanghera et al., 2012; Craciunescu et al., 1999; Dettori and Semler, 2007; Al-Kadi, 2010). Statistical-based techniques have been

most commonly applied and describe the distribution and relationships of intensity-level values in the image. Three orders of parameters are described in statistical-based texture analysis (Craciunescu et al., 1999; Dettori and Semler, 2007; Al-Kadi, 2010).

First-order statistics relate to intensity level frequency distribution within the region of interest, which can be obtained from the histogram of pixel intensities. It is dependent on a single pixel value rather than its interaction with neighboring pixels (Tuceryan and Jain, 1998). *First order* statistics based on histogram analysis include intensity (mean, minimum and maximum), uniformity, skewness and kurtosis. Second-order statistics are co-occurrence measurements calculated using spatial gray-level dependence matrices. These matrices determine how often a pixel of intensity *i* finds itself within a certain relationship to another pixel of intensity *j*. *Second-order* statistics based on a co-occurrence matrix (GLCM) include entropy, homogeneity, dissimilarity and correlation (Tuceryan and Jain, 1998). *Higher-order* statistics are calculated using neighborhood gray-tone-difference matrices, which examine the spatial relationship among three or more pixels (Amadasun and King, 1989; Srinivasan and Shobha, 2008). This is calculated using the neighborhood gray-tone-difference matrix (NGTDM). Examples of higher-order statistics include contrast, coarseness and busyness.

Numerous studies show the positive outcome of textural heterogeneity analysis. Several hundred published articles have investigated the beneficial information that can be extracted from the analysis of tumor heterogeneity. More than 70 percent of articles involve MR and ultrasonography. Since the last decade the interest in exploring tumor heterogeneity using PET has gained momentum and is being explored worldwide owing to a great role of PET in oncology. One such study was conducted by Bundschuh et al (Bundschuh et al., 2014). Aim of this study was to investigate the predictive and prognostic value of tumor heterogeneity assessed in FDG PET-CT in patients with colorectal cancer treated with neoadjuvant radiochemotherapy using histopathology as gold standard and clinical follow up. Assessment of tumor heterogeneity was performed using coefficient of variation (COV), skewness and kurtosis. For comparison, the conventional PET parameters

such as SUV (standard uptake value), tumor volume and maximum diameter were used. Results showed that COV showed best predictive capability for histopathologic response. COV in pre-therapeutic PET also showed significant prognostic capability for progression free survival. Similarly, in another study conducted by Pyka et al (Pyka et al., 2015) the objective was to investigate the predictive and prognostic value of the textural heterogeneity parameters in FDG PET-CT before start of stereotactic radiotherapy in non-small cell lung carcinoma with long-time follow-up for comparison. In the results two parameters entropy and correlation showed the best predictive capability for local recurrence and also for predicting long term survival.

We carried out this study as an effort to improving the diagnostic accuracy of PET-CT by the use of textural heterogeneity parameters. The presented work comprises of three parts. In the first part we used textural heterogeneity parameters in the differentiation of pseudoprogression from real progression in high grade glioma patients using FET (flouro ethyl tyrosine) PET. In the second part of our study we studied the role of textural heterogeneity parameters for patient selection in ^{177}Lu-PSMA (prostate specific membrane antigen) therapy via ^{68}Ga-PSMA PET. In the third part of our study we studied the role of textural heterogeneity parameters for therapy response assessment and prognosis in prostate cancer patients undergoing ^{177}Lu-PSMA therapy.

1.3 Role of textural heterogeneity parameters in diagnosis of pseudoprogression in high grade gliomas

The objective of this study was to distinguish between true tumor progression and pseudoprogression in the patients of high grade glioma using textural heterogeneity parameters in FET-PET as compared to the conventional PET parameters.

The management of high grade gliomas (HGG) is very complex. The standard options available for treatment include surgery followed by chemotherapy and radiotherapy. Numerous factors put a direct influence on the selection of appropriate treatment option.

These include age, performance status of patient, histological type of the tumor ad its grade. The gold standard for follow up us is magnetic resonance imaging (MRI) However, in numerous cases it becomes really difficult to differentiate between the treatment response and the tumor effect. However, this distinction is very essential for further planning of therapy. Different diagnostic methods being utilized to get best possible results including proton spectroscopy, dynamic imaging with contrast enhanced MRI and amino acid radiotracer imaging (Khan et al., 2016).

Gliomas can be highly malignant tumors that originate from the glial cells or their precursors in the central nervous system. They comprise of the major chunk of all malignancies of the central nervous system. The current World Health Organization histologic classification system uses histopathologic changes of cellular atypia, mitotic activity, endothelial cell proliferation, and necrosis to classify gliomas as “low grade” (grades I and II) and “high grade” (grades III and IV) (Louis et al., 2007). Despite state-of-the-art surgery, radiation therapy and chemotherapy, the prognosis of patients with high-grade glioma is grim. In patients with the most aggressive and devastating form of high grade gliomas, glioblastoma, median overall survival is about 17 months.

Pseudoprogression can be defined as new areas of enhancement or edema that do not arise from actual tumor progression, but from chemoradiotherapy related inflammation, which is likely because of increased vascular permeability (Brandsma et al., 2008). This phenomenon of pseudoprogression was recognized as early as 1979 (Hoffmann et al., 1979). To this day pseudoprogression poses a great clinical challenge because its appearance at imaging is indistinguishable from that of true disease progression. Before the use of Temozolomide (TMZ) chemoradiation, only approximately 1% of patients treated with focal fractional radiotherapy alone would develop treatment-related imaging changes (Chaskis et al., 2009). However, with the current regimen, pseudoprogression been reported in up to 50% of patients, typically noted at the first follow-up MRI obtained within 2–3 months after chemoradiation therapy (Taal et al., 2008).

Failure to identify pseudoprogression can lead to various negative outcomes directly affecting the morbidity and mortality of the patient. It can result in unnecessary surgical interventions or excessive chemotherapy. It can also result in premature termination of treatment. As pseudoprogression is a transient phenomenon occurring as a side effect of chemoradiation, it has the capability of spontaneous resolution. This spontaneous resolution can also give the false impression that therapy is effective. So, it is very essential to differentiate it from the actual tumor progression. On the other hand, successful differentiation of pseudoprogression from actual tumor progression can lead to an improvement in prognosis, possibly because of the increased likelihood of O^6-methylguanine-DNA-methyltransferase (MGMT) gene promoter methylation in this population (Gahramanov et al., 2014).

In response to the accumulative evidence regarding the role of pseudoprogression in deciding treatment modifications, the Response Assessment in Neuro-Oncology (RANO) criteria provided an update in 2010 to account for the phenomenon of pseudoprogression (Wen et al., 2010). The RANO criteria specifies that, within the first 12 weeks after completion of radiotherapy, tumor progression can be established only if most of the new enhancement occurs outside the radiation field or if histologic confirmation of progression is obtained. However, a diagnostic dilemma remains for enlarging enhancement and peritumoural edema that occurs within the radiation field during the initial 12 weeks. Biopsy samples can sometimes reveal either obvious tumor growth or therapy-induced changes, but in many instances, even histologic assessment fails to resolve the dilemma because of sampling errors, inconclusive specimens with mixed treatment and tumor histologic findings, inter-observer variability, and inconsistent definitions of residual and recurrent disease (Melguizo-Gavilanes et al., 2015).

Currently the diagnosis of pseudoprogression is built on increasing contrast enhancement on MRI. When an increasing contrast-enhancing lesion on MRI indicates pseudoprogression, the current gold standard is to perform follow-up MRIs to evaluate

changes in lesion size. Consequently, a diagnosis of pseudoprogression can only be made retrospectively based on follow-up MRI. It would be, however, advantageous for patient management if pseudoprogression could be identified at the earliest possible time point when the increasing contrast-enhancing lesions are detected for the first time. This is particularly important for patients with greatly increasing contrast-enhancing lesions and deteriorating clinical status. These patients might not be able to wait 4-8 weeks for a follow-up MRI to decide whether secondary surgery or any other therapeutic adjustments are necessary.

To make an effective and timely diagnosis of pseudoprogression different treatment modalities are being used, among them positron emission tomography is very effective. In cases of true progression there is increased radiotracer accumulation the lesions as compared to pseudoprogression. More important of these are the imaging techniques involving radiotracers other than conventional 18-flourodeoxygenase (FDG) PET as its application is limited owing to high glucose metabolic state of the normal brain tissue resulting in a decreased signal to noise ratio. FDG PET also shows an increased uptake in inflammatory cells which can hinder the diagnosis of actual tumor. There is increased protein synthesis in brain tumors making amino acid radiotracers as an effective mode of imaging. In a study evaluating 72 patients with ^{11}C–methionine PET, a threshold uptake index of 9 could distinguish between true tumor progression and pseudoprogression with 83.5% sensitivity and 97% specificity (Skvortsova et al., 2014). A smaller study using PET imaging with the amino acid tracer *O*-2-^{18}F-fluoroethyl-L-tyrosine and a cut-off value of 2.3 demonstrated 100% sensitivity and 91% specificity in discriminating true tumor proliferation from pseudoprogression (Galldiks et al., 2014). In the recent years use of ^{18}F-FET PET has been increased a lot in brain tumor imaging. The rapid accumulation of FET in brain tissue is independent of blood brain barrier disruption as compared to MRI where contrast enhancement can cause reactive changes to blood brain barrier which can then mimic tumor progression.

In a study (Galldiks et al., 2015) the aim was to assess the clinical value of ^{18}F-FET PET in the differentiation of pseudoprogression (PsP) and early tumor progression (EP) after radiochemotherapy of glioblastoma. A group of 22 glioblastoma patients with new contrast-enhancing lesions or lesions showing increased enhancement (>25 %) on standard MRI within the first 12 weeks after completion of radiochemotherapy with concomitant temozolomide (median 7 weeks) were additionally examined using amino acid PET with ^{18}F-FET. Pseudoprogression was confirmed in 11 of the 22 patients. In patients with pseudoprogression, ^{18}F-FET uptake was significantly lower than in patients with early tumor progression and presence of MGMT promoter methylation was significantly more frequent ($P = 0.05$). It was concluded that ^{18}F-FET PET may facilitate the diagnosis of pseudoprogression following radiochemotherapy of glioblastoma. In another study (Rachinger et al., 2005) the objective was to analyze the diagnostic value of FET-PET and MRI in the detection of tumor recurrence in patients with glioma after radiotherapy, radiosurgery, or multimodal treatment. Results showed that Specificity of FET-PET was 92.9%, and sensitivity was 100% (in patients suspected of having recurrent tumor as revealed by MRI). Sensitivity of MRI was 93.5%, and specificity was 50% ($P < 0.05$). It was concluded that for patients with gliomas undergoing multimodal treatment or various forms of irradiation, conventional follow-up with MRI is insufficient to distinguish between benign side effects of therapy and tumor recurrence. FET-PET is a powerful tool to improve the differential diagnosis in these patients.

Similarly, role of tumor textural heterogeneity has been evaluated in various brain tumors including gliomas, but most of the times it has been based on MRI. In a recent study by (Liu et al., 2017) the aim was to assess the glioblastoma heterogeneity with MR imaging textures and to evaluate its impact on survival time. The results suggest that local and regional heterogeneity may play an important role in the survival stratification of patients with glioblastoma. The top 10 features included 7 run-length matrix and 3 co-occurrence matrix features, in which all 6 regional run-length matrix features emphasizing high gray-levels ranked in the top 7. In another study by (Molina et al., 2016) the objective was to analyze three-dimensional (3D) heterogeneity measures of post-contrast pre-operative MR

images acquired with T_1 weighted sequences of patients with glioblastoma as predictors of clinical outcome. Results showed that 4 of the 11 run length matrix features and 4 of the 5 co-occurrence matrix features considered were robust predictors of survival. The median survival differences in the most significant cases were of over 6 months. It was concluded that heterogeneity measures computed on the post-contrast pre-operative T_1 weighted MR images of patients with glioblastoma are predictors of survival.

In the study we carried out, the aim was to distinguish between pseudoprogression and real tumor progression in high grade glioma patients using textural heterogeneity parameters. The heterogeneity parameters were assessed in FET-PET images. The purpose of the study was to enable an earlier diagnosis of pseudoprogression which can help in therapy planning and thus directly affecting the survival outcome of patients, as the delay in this diagnosis can cause over or under treatment of patients. Fourteen patients with high grade glioma and suspected of pseudoprogression underwent FET-PET imaging. A set of 19 conventional and textural FET-PET features were evaluated and subjected to unsupervised consensus clustering. The final diagnosis of true progression versus pseudoprogression was based on follow-up MRI using RANO criteria.

1.4 Role of textural heterogeneity parameters in patient selection for ^{177}Lu-PSMA therapy

The objective of this study was to assess predictive ability of tumor textural heterogeneity parameters from baseline ^{68}Ga-PSMA PET prior to ^{177}Lu-PSMA therapy in hormone refractory metastatic prostate cancer patients.

In the European Union, prostate cancer is ranked first among the most frequently diagnosed cancer among men, with around 345,000 new cases estimated in 2012. Prostate cancer accounted for 24 per cent of all new cancers in the same year. For 2015 the estimated number of new prostate cancer cases was about 365,000 (Crocetti Emanuele,

2015). Prostate cancer tends to be highly aggressive and can lead to significant mortality by causing death of more than 250.000 men each year (Lozano et al., 2012). For many years there were few options for treatment of metastatic prostate cancer. The ones available usually involved the use of androgen deprivation agents. However, there is continuous development of new and more effective agents for tackling prostate cancer. It is under persistent surveillance worldwide by physicians and researchers and it is of utmost importance to devise new methods aiming for earlier diagnosis and optimum individualized therapy of prostate cancer.

Among the ongoing advancements for the treatment of prostate cancer the possibilities involving Prostate Specific Membrane Antigen (PSMA) as an optimal diagnostic and therapeutic marker have gained momentum. PSMA is a type II membrane protein originally characterized by the murine monoclonal antibody (mAb) 7E11-C5.3 and is expressed in all forms of prostate tissue, including carcinoma (Ross et al., 2003; Horoszewicz et al., 1987). Significant overexpression is seen in metastatic, hormone refractory and poorly differentiated carcinomas. Studies have consistently demonstrated PSMA expression in all types of prostate tissue and increased PSMA expression in cancer tissue (Silver et al., 1997; Troyer et al., 1995; Chang et al., 2011). Bostwick and colleagues (Bostwick et al., 1998) described PSMA immunohistochemical expression in 184 prostate specimens examined, all of which had PSMA expression and demonstrated a correlation between this expression and severity of cancer. There was an increase in the percentage of PSMA staining from benign epithelial tissue (69.5% of cells positive) to high-grade prostatic intraepithelial neoplasia (77.9% of cells positive) to malignant cells (80.2% of cells positive).

The five year survival rate of locally advanced prostate cancer is nearly 100%; however, the rate is significantly lower in the case of metastatic disease (31%) (Jemal et al., 2010). Therefore, developing new strategies for diagnosis, imaging, and treatment of metastatic prostate cancer is of major importance. As discussed earlier prostate specific membrane antigen serves as an ideal target for therapy especially for metastatic disease. Radiolabeled ligands targeting PSMA have recently been the subject of numerous studies

showing high sensitivity and contrast in detecting recurrent prostate cancer and its metastases with remarkable detection rates (Afshar-Oromieh et al., 2013; Eiber et al., 2015). Recent studies have also shown a high sensitivity of PSMA-targeted imaging in determining the local extent of disease before radical prostatectomy (Rahber et al., 2016; Eiber et al., 2016). Benesová et al (Benesová et al., 2015) introduced a high-affinity PSMA ligand (PSMA-617) that can be labeled with ^{68}Ga or ^{177}Lu and demonstrates superior tumor-to-background uptake.

In order for therapy to become effective it is very essential to be able to select patients who can benefit most from therapy. It can serve as a basis of personalized medicine. This optimal patient selection can help transform the treatment options for patients depending on their response. As earlier in the course of therapy the efficacy of the treatment is predicted the more beneficial is the outcome. One approach is trying to deduce information from the pre-therapy scan. This is of great importance because some valuable data can be obtained even before the start of therapy. Patient selection can be made and patients can be assigned in various groups based on predicted responsiveness to available treatment options. A lot of data is available on evaluation of pre-therapy scans. Different parameters have been used to extract useful information from pre-therapy scans. As our research is based on the role of tumor textural heterogeneity parameters, we paid emphasis to studies which involved the use of textural heterogeneity parameters for evaluation of pre-therapy scans for patient selection and response prediction.

In a study by Eary JF et al. (Eary et al., 2008) the aim was to support the hypothesis that a new heterogeneity-analysis algorithm applied to ^{18}F-FDG PET images of tumors in sarcoma patients is predictive of patient outcome. ^{18}F-FDG PET images from 238 patients with sarcoma were analyzed using a new algorithm for heterogeneity analysis in tumor ^{18}F-FDG spatial distribution. Statistical analyses show that heterogeneity analysis is a strong independent predictor of patient outcome. Cheng NM et al. (Cheng et al., 2013) sought to investigate whether the textural features of pretreatment ^{18}F-FDG PET-CT images can provide any additional prognostic information over TLG and clinical staging in patients with

advanced T-stage oropharyngeal squamous cell carcinoma (OPSCC). Study involved the retrospective analysis of pretreatment ^{18}F-FDG PET-CT images of 70 patients. The textural features of pretreatment ^{18}F-FDG PET-CT images were extracted from histogram analysis, normalized gray-level co-occurrence matrix and neighborhood gray-tone difference matrix. It was concluded that uniformity extracted from the normalized gray-level co-occurrence matrix represents an independent prognostic predictor in patients with advanced T-stage OPSCC. Similarly, in another study by Pyka T et al. (Pyka et al., 2015) evaluated the predictive value of textural heterogeneity parameters in pre-treatment FDG –PET scans for recurrence and prognosis in NSCLC patients receiving primary stereotactic radiation therapy (SBRT). Entropy (AUC 0.872) predicted local recurrence. In another very interesting study by Tixier F et al. (Tixier et al., 2011) aim was to propose and evaluate new parameters obtained by textural analysis of baseline PET scans for the prediction of therapy response in esophageal cancer. Different image-derived indices obtained from the pretreatment PET tumor images included usual indices such as maximum SUV, peak SUV, and mean SUV and a total of 38 features extracted from the 5 different textures. It was concluded that textural features of tumor metabolic distribution extracted from baseline ^{18}F-FDG PET images allowed for the best stratification of esophageal carcinoma patients in the context of therapy-response prediction.

These studies show that textural heterogeneity parameters can play a role in outcome prediction and as it can be seen from the abovementioned studies, very useful information can be gained from pre-therapy scans only, hence resulting in earliest possible options for treatment modifications in order to get better response. However, there is no data available explaining the role of textural heterogeneity from baseline ^{68}Ga-PSMA scans. PSMA is now being widely used as a therapeutic agent in the form of ^{177}Lu-PSMA (it will be discussed in detail in the next part) and this therapy has a very good response rate. Still some recent studies found a non-responder rate of about 30% (no PSA decline) after radiopeptide therapy with ^{177}Lu-PSMA (Ferdinandus et al., 2017; Ahmadzadehfar et al., 2017; Rahbar et al., 2016; Rahbar et al., 2017).

The objective of this current study was hence to assess the predictive ability of tumor textural heterogeneity parameters from baseline ^{68}Ga-PSMA PET scan. Selected textural heterogeneity parameters had been previously widely used in different studies and showed a significant potential for depicting the outcome (Pyka et al., 2015; Tixier et al., 2011; Dong et al., 2016; Dong et al., 2015). The predictive value of these parameters was compared to established clinical parameters (Prostate specific antigen (PSA), serum and bone alkaline phosphate, eastern cooperative oncology group (ECOG) criterion). The aim of the study was to help in patient selection prior to ^{177}Lu-PSMA therapy in an order to enhance the efficacy of therapy for responders which were determined from the baseline scans.

1.5 Role of Tumor Textural Heterogeneity in ^{68}Ga-PSMA PET-CT for Therapy Response Assessment and Prognosis in Prostate Cancer Patients

The last part of our study comprised of the assessment of role played by tumor textural heterogeneity parameters in prostate cancer patients undergoing ^{177}Lu-PSMA therapy for assessing the response to therapy and prognosis of the patients.

Since last three to four years, special emphasis is being paid to treatment of hormone refractory prostate cancer with ^{177}Lu-PSMA therapy. Several studies reported promising results for response rates and a favorable safety profile after radioligand therapy (RLT) with ^{177}Lu-PSMA-617 in patients with metastatic castration-resistant prostate cancer (mCRPC) (Ahmadzadehfar et al., 2015; Kratochwil et al., 2016: Rahbar et al., 2016a, 2016b; Ahmadzadehfar et al., 2016). In order to further strengthen these results, a retrospective multicenter study was initiated by the German Society of Nuclear Medicine in July 2015 (Rahbar et al., 2017). Twelve therapy centers retrospectively collected and pooled data on safety and efficacy of ^{177}Lu-PSMA-617 RLT. This retrospective multicenter study aimed at analyzing the optimal dose and number of therapy cycles and predictors of response in more detail. This study demonstrated the favorable safety and efficacy of ^{177}Lu-PSMA-617 RLT in a large number of mCRPC patients and stated that ^{177}Lu-PSMA-617

RLT might exceed the performance of other third-line systemic therapies reported in the literature. In the light of published data it could be deduced that radioligand therapy (RLT) with Lu-177 PSMA is effective and had a low toxicity profile (Kratochwil et al., 2016). It was also observed that up to 30% of patients did not show prostate specific antigen (PSA) decline in response to RLT (Kratochwil et al., 2016; Zechmann et al., 2014).

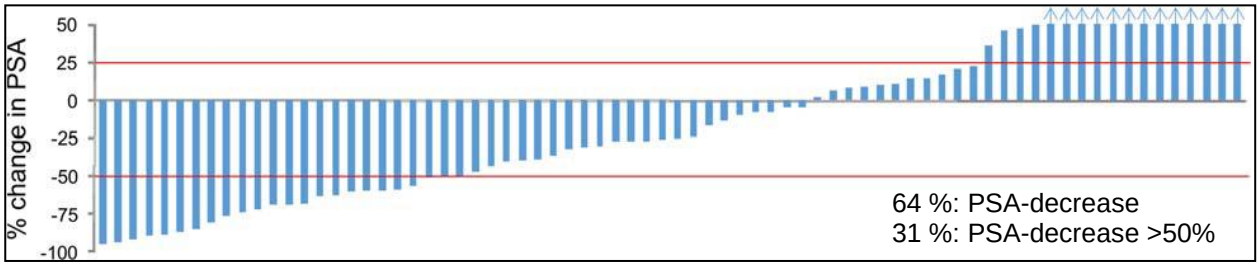

ill. 3 Results of German multicenter study investigating ^{177}Lu-PSMA-617 radioligand therapy in advanced prostate cancer patients (Rahbar et al., 2017)

The therapy showed good response rate but in order to improve the efficacy of treatment for non-responsive patients, it is essential to devise some techniques which can help in better assessment of individual patient behavior. In our study, we aimed to analyze the role of textural heterogeneity parameters for therapy response assessment. Textural heterogeneity parameters have been used several times to assess the response of a tumor to therapy. In the study performed by Bundschuh et al. (Bundschuh et al., 2014) the objective was to analyze the capability of textural inhomogeneity markers on PET to predict histopathologic therapy response and outcome in patients with locally advanced rectum carcinoma treated with neoadjuvant radiation chemotherapy. Twenty-seven patients underwent ^{18}F-FDG PET-CT before, 2 week after the start, and 4 week after the completion of neoadjuvant chemoradiotherapy. Convention PET parameters and tumor textural heterogeneity parameters were assessed in each scan. The results showed that a textural heterogeneity parameter COV (coefficient of variation) had statistically significant capability

to assess histopathologic response early in therapy (sensitivity, 68%; specificity, 88%) and after therapy (79% and 88%, respectively). It was concluded that tumor heterogeneity assessed by the COV, being superior to the investigated conventional parameters, is an important predictive factor in patients with rectal cancer. Furthermore, it can provide prognostic information. Therefore, its application is an important step for personalized treatment of rectal cancer. Similarly, Lapa C et al. analyzed in a study (Lapa et al., 2015) the potential of somatostatin receptor subtype II (SSTR) PET to assess intraindividual tumor heterogeneity and thereby treatment response prior to peptide receptor radionuclide therapy (PRRT). 12 patients with progressive radioiodine-refractory differentiated thyroid cancer were enrolled in the study. Conventional PET parameters and heterogeneity parameters were analyzed regarding their potential to predict progression-free (PFS, mean, 221 days) and overall survival (OS, mean, 450 days). In patient-based analysis, all conventional parameters failed to predict PFS. Several textural parameters showed a significant capability to assess PFS. Thereby, "Grey level non uniformity" had the highest area under the curve (AUC, 0.93) in Receiver operating characteristics analysis followed by "Contrast" (AUC, 0.89). In lesion-based analysis, only "Entropy" revealed potential to evaluate disease progression. It was concluded that tumor textural heterogeneity seems to be a predictor of response to PRRT in patients with iodine-refractory differentiated/advanced medullary thyroid cancer and outperforms conventional PET parameters like standardized uptake value.

The purpose of our study was to investigate the role of tumor heterogeneity in the assessment of therapy response on pre therapeutic (baseline) ^{68}Ga-PSMA PET, as well as to monitor changes during the course of ^{177}Lu-PSMA therapy by analyzing the mid-therapy and post-therapy scans as well. Every patient went under three ^{177}Lu-PSMA therapies. Conventional and textural parameters were thoroughly analyzed in all PET scans. The gold standard was the serum PSA level. The changes in serum PSA level correlate with overall survival in castration resistant metastatic prostate cancer at showed by a recent study (Ahmadzadehfar et al., 2017). In addition to evaluating the predictive value of tumor

heterogeneity, we also analyzed the prognostic value for disease progression and overall survival.

In the nutshell, our study aimed at the improvement in specificity of PET signals by the analysis of tumor textural heterogeneity parameters. This was performed in an effort to enhance the diagnostic accuracy of PET scans. In many instances the conventional PET parameters e.g. SUV, tumor volume are not able to give optimal information. Textural heterogeneity parameters are proving to be a better alternative for assessment. As seen from a large number of studies textural heterogeneity parameters are fast establishing their role in many aspects of diagnostic and therapeutic nuclear medicine. They are being widely used to predict response from baseline scans. This is of great importance, because useful analysis in baseline scans can give earliest possible insights into tumor behavior and therapy response prediction. It can help in selection of patients who can benefit from treatment and can also help to modify the therapy for otherwise nonresponsive patients thus not only improving the efficacy of therapy but also decreasing the disease burden of patient. Similarly, role of heterogeneity parameters is also seen in scans over the course of therapy to predict the prognosis and survival outcome of patients. They can also help distinguish pathology from reactive changes much more effectively than conventional parameters. All this has been discussed in abovementioned and many other studies.

Role of textural heterogeneity parameters in FET-PET to distinguish pseudoprogression in high grade gliomas and their importance in PSMA therapy is the subject of our study. These scenarios have not been explored before and our study showed some very good outcomes which will be discussed in detail in the following sections.

2. Materials and Methods

As our study has been divided into three parts the material and methods will be discussed in accordance.

2.1 Role of textural heterogeneity parameters in diagnosis of pseudoprogression in high grade gliomas

2.1.1 Patient selection

For this retrospective analysis, the patient files of the Division of Clinical Neuro-oncology were searched for histologically confirmed high-grade glioma (HGG) patients meeting the following characteristics:

(1) Patients experiencing increasing contrast-enhancing lesions on MRI (+25% in two perpendicular diameters) and/or any new lesion according to RANO (Wen et al., 2010) (minimum lesion size >10 mm) more than 4 weeks after the end of radiotherapy,
(2) Patients having a routine FET-PET following detection of increasing contrast-enhancing lesions,
(3) After initial MRI and FET-PET, a further contrast-enhanced MRI ensued at least 4 weeks later without change of therapy. O-6-methylguanine-DNA methyltransferase (MGMT) promoter methylation status was tested using pyrosequencing (Mikeska et al., 2007).

2.1.2 PET Imaging with ^{18}F-FET

Data were acquired with a Biograph Sensation 2 PET-computer tomography (PET-CT) scanner (Siemens Medical Solutions). The axial and transverse fields of view were

16.2 and 58.5cm respectively. The transverse resolution of the scanner was about 6.5mm, whereas the axial resolution was 6.0mm, both at a radius of 10mm. The computer tomography (CT) component was a 2-slice spiral CT scanner. About 60 minutes after the intravenous injection of approximately 200 MBq of FET, the patient was placed in the scanner. Low dose CT of the head (caudocranial) was performed followed by the PET scan of the same area in a single bed position. The CT data were reconstructed in 512 x 512 pixel matrices. PET data was reconstructed into 256 x 256 matrices using the iterative attenuation-weighted ordered subset algorithm implemented by the manufacturer using 4 iterations and 16 subsets. Attenuation and scatter correction was performed using the CT data. Final voxel size was 5.3mm x 5.3mm x 5mm. All patients gave written and informed consent to the imaging procedure.

2.1.3 PET Data Analysis

Image data were transferred to an Interview Fusion Workstation (Mediso Medical Imaging System, Budapest, Hungary). Firstly, co-registration between PET and CT images was performed. Tumor volume was manually delineated on PET images. For background assessment 5 ROIs with a fixed diameter of 15mm were placed on normally appearing cortex area, 2 on the frontal lobe, 2 on the occipital lobe and 1 on the contralateral region to the tumor. A mean value was then calculated for these ROIs. In addition, a semiautomatic segmentation in PET was performed based on background activity for which tumor delineation cutoff was taken as 1.6 times the mean value of background ROIs.

For assessment of tumor uptake heterogeneity additional 13 textural heterogeneity PET parameters were estimated, namely, Coefficient of Variation (COV), Entropy, Correlation, Contrast, Size-zone Variability (Size variation), Intensity Variability (Intensity variation), Morphologic Volume of the Lesion (Volume), Coarseness, Complexity, Short Zone Emphasis (Short Zone Emphasis), Long Zone Emphasis (Long zone Emphasis), Zone Percentage, Short Run Emphasis (Short Run Emphasis), and Long Run Emphasis (Long Run Emphasis).

PET Feature	Explanation
Correlation	A measure of continuous areas of same or similar voxel values in an image. An image with high correlation values is usually associated with large areas of similar uptake intensities.
Coarseness	A measure of the intensity differences throughout the image.
COV	A normalized measure of dispersion of a frequency distribution (standard deviation divided by the mean value of the activity concentration in the tumor volume).
Contrast	A measure of local variations present in the image. A high contrast value indicates a high degree of local variation.
Complexity	Measures the uniformity of patterns versus rate of change in an image.
Entropy	Measures randomness of distribution, e.g. a homogenous matrix demonstrates low entropy.
Size Variation	Measures the difference of the grey value when going to the next voxel. It is high when the intensity changes very often between single voxels.
Intensity Variation	The intensity variation describes the variation of the intensity of different substructures.
Short Run Emphasis	Measure of consecutive pixels which have the same gray level intensity along a specific linear orientation. Fine textures tend to contain more short runs with similar gray level intensities.
Long Run Emphasis	Measure of consecutive pixels which have the same gray level intensity along a specific linear orientation. Coarse textures have more long runs with significantly different gray level intensities
Short Zone Emphasis	Measures the distribution of short zones as the difference of the grey value when going to the next voxel. It is high when the intensity changes very often between single voxels.
Long Zone Emphasis	Measures the distribution of long zones as the difference of the grey value when going to the next voxel.
Zone Percentage	Measures the percentage of zones of a given size.
SUV Mean	A measure of mean radiotracer accumulation in tumor lesions.
SUV Max	A measure of maximum radiotracer accumulation in tumor lesions.
TNR Mean	Mean tracer uptake in the tumor divided by that in normally appearing brain tissue.
TNR Max	Maximal tracer uptake in the tumor divided by that in normally appearing brain tissue.
TLG	The total lesion volume and its metabolic activity
Volume	The total lesion volume

Table 1: Overview of textural heterogeneity parameters

All parameters were assessed in 3-dimensional volumes. In addition, the following 6 conventional PET parameters were evaluated: mean SUV (Mean), maximum SUV (Max), Total Lesion Glycolysis (TLG), mean tumor to background ratios (TNRmean) and maximum tumor to background ratios (TNRmax). Their overview is shown in table 1.

2.1.4 Diagnosis of True Progression

The diagnosis of tumor progression was made when progressive contrast-enhancing lesions according to RANO criteria (Wen et al., 2010) were noted on initial MRI and when further progression of contrast-enhancement ensued on a follow-up MRI at least 4 weeks later. By contrast, the diagnosis of pseudoprogression was applied when the follow-up MRI showed stabilization or regression of the contrast-enhancing lesions, provided that neither clinical worsening nor change in treatment ensued in the interim. In all patients, MRI scan analysis was carried out by an experienced neuroradiologist and another independent investigator.

In the event of true progression, progression-free survival (PFS) was defined as the time elapsed between the date of the true tumor progression (retrospectively defined as the date of the initial MRI conducted immediately before PET) and the date of the subsequent progression defined by MRI. In the event of pseudoprogression, PFS was defined as the time between the date of initial MRI conducted immediately before PET and the date of subsequent MRI defining progression.

2.1.5 Subtype discovery

Unsupervised consensus clustering was used for class discovery to uncover groups of items sharing FET-PET characteristics. Consensus clustering is a class discovery technique for the detection of unknown possible clusters consisting of items with similar intrinsic features (Wilkerson and Hayes, 2010). Being distinct from conventional clustering methods, it provides quantitative evidence to determine the number and membership of

clusters. To apply this method on our dataset, we first standardized FET-PET features to obtain z-scores. This was followed by subsampling 80% of items and PET features 10 000 times and partitioning each subsample up into k=7 groups by the agglomerative hierarchical clustering algorithm using Pearson correlation distance. For each k, a consensus matrix was filled with consensus values, defined as the proportion of clustering repetitions in which two items are classified together. To determine the optimal number of k, we drew upon empirical cumulative distribution function (CDF) plots to find the k at which the distribution reached an approximate maximum, indicating a maximum stability. To validate the so obtained optimal number of clusters, we applied the proportion of ambiguous clustering (PAC) method (Wilkerson and Hayes, 2010).

To identify a minimal subset of PET features that succinctly characterizes each cluster we used the nearest shrunken centroids method called predictive analysis of microarrays (PAM) (Wilkerson and Hayes, 2010). To this end, we used 10-fold cross-validation to determine the amount of shrinkage at which the error rate was minimized.

2.1.6 Statistical analysis

To assess cluster stability in our unsupervised analysis, along with performing consensus clustering over 10 000 iterations we used the CDF and CDF progression graphs to detect the optimal number of clusters. Furthermore, we relied on PAC to confirm our choice. To compare clinical and molecular data across clusters, we used the Kruskal-Wallis test for continuous variables and the Fisher's exact test for categorical variables. Moreover, logistic regression and Fisher's exact test for 2 x 2 contingency tables were performed to assess the association of pseudoprogression with cluster assignments. A p-value below 5% was considered significant. Statistical analysis was carried out using Stata (release 14.0; StataCorp LP) and R Statistical Software (version 3.2.4).

2.2 Role of textural heterogeneity parameters in patient selection for ^{177}Lu-PSMA therapy

2.2.1 Patient selection

70 patients with histologically proven prostate cancer were retrospectively included in this study. Clinical data was collected from November 2014 to April 2016. All patients were planned to undergo ^{177}Lu-PSMA-617 (abbreviated as ^{177}Lu-PSMA in this study) radioligand therapy. Average age of patients was 71.46 years. Inclusion criteria for this retrospective analysis were progressive metastatic castration-resistant prostate cancer (mCRPC) patients. Patients experienced progression under next-generation androgen-deprivation therapy (e.g., abiraterone, enzalutamide) or first- or second-line chemotherapy (e.g., docetaxel, cabazitaxel) or were not eligible for chemotherapy. All patients eligible for ^{223}Ra received this treatment before undergoing ^{177}Lu-PSMA-617 radioligand therapy. 39 patients had prior chemotherapy. 16 patients had been treated previously with ^{223}Ra, while 27 patients had previous external beam radiation therapy (EBRT).

2.2.2 ^{68}Ga-PSMA Scan

A ^{68}Ga-PSMA-617 (abbreviated in this study as ^{68}Ga-PSMA) PET scan was performed for every patient. Each patient underwent ^{68}Ga-PSMA scan before therapy with ^{177}Lu-PSMA termed as the baseline scan. The objectives of the baseline scan included staging and therapy planning. After the baseline scan patients underwent ^{177}Lu-PSMA radioligand therapy. Renal function of every patient was analyzed prior to therapy with ^{99m}Tc-MAG3 renal scintigraphy. Patient characteristics are shown in table 2.

Characteristic	Data
Age	71.46 years (48-88years)
Site of metastasis:	
Bone	70 (100%)
Lymph node	33 (47.1%)
Other (liver, prostate)	15 (21.4 %)
Previous therapy of mCRPC:	
Androgen deprivation therapy	70 (100%)
Chemotherapy	39 (55.7%)
^{223}Ra	16 (22.8%)
EBRT to bone	27 (38.5%)

Table 2: Patient characteristics

Data were acquired with a Biograph Sensation 2 PET/computer tomography (PET/CT) scanner (Siemens Medical Solutions). The axial and transverse fields of view were 16.2 and 58.5cm respectively. The transverse resolution of the scanner was about 6.5mm, whereas the axial resolution was 6.0mm, both at a radius of 10mm. The computer tomography (CT) component was a 2-slice spiral CT scanner. About 73 minutes (range 50-90 minutes) after the intravenous injection of approximately 131.3 MBq (range 98.8 to 174.8 MBq) of ^{68}Ga-PSMA, the patient was placed in the scanner. Low dose CT from the head to mid-thighs was performed followed by the PET scan of the same area in 6-7 bed positions, each for 3-4 minutes depending on the body weight of the patient. The CT data were reconstructed in 512 x 512 pixel matrices. PET data was reconstructed into 128 x 128 matrices in axial, coronal and sagittal planes using the iterative attenuation-weighted ordered subset algorithm implemented by the manufacturer using 4 iterations and 16 subsets. Attenuation and scatter correction was performed using the CT data. Final voxel size was 5.3mm x 5.3mm x 5mm. All patients gave written and informed consent to the imaging procedure. All patient record and information was anonymized before analysis.

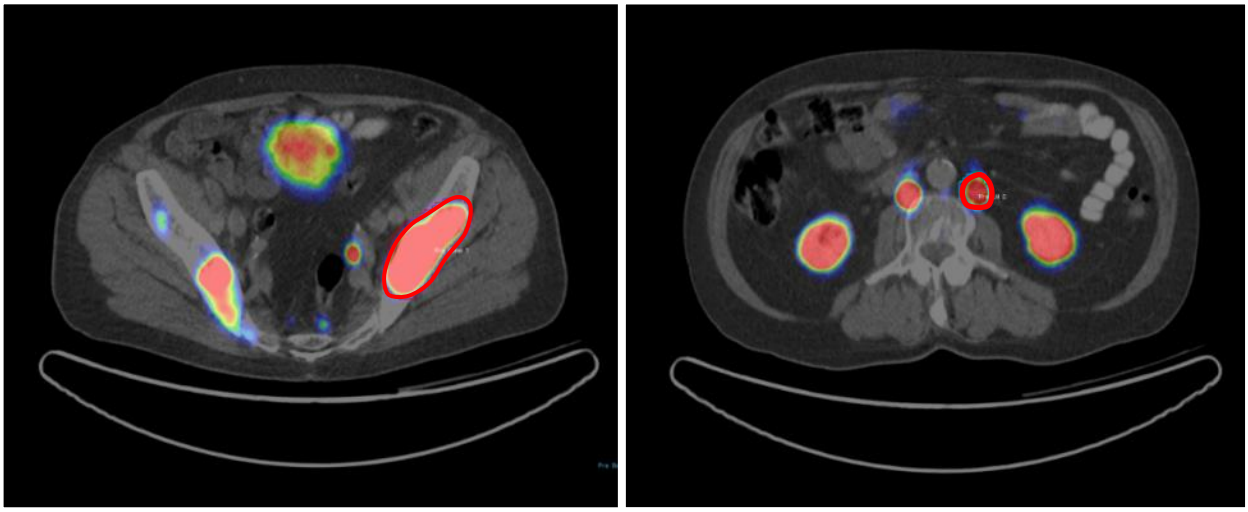

ill. 4: ROIs for analysis of bone and lymph node lesions

2.2.3 PET Data Analysis

Image data were transferred to an Interview Fusion Workstation (Mediso Medical Imaging System, Budapest, Hungary). Firstly, co-registration between PET and CT images was performed. Tumor volume was manually delineated on PET images (Figure 1) with a standard uptake value (SUV) threshold (Fendler, 2017; Mathieu, 2015). All the 70 patients had bone metastasis. Thirty three patients had lymph node metastasis along with bone metastasis. Fifteen patients had additional liver and/or prostate lesions. Three VOIs each for bone and lymph node lesions were delineated manually. Other lesions were also delineated if present in liver and prostate. Parameters to be evaluated were measured in these VOIs. A total of 328 VOIs were delineated. Mean volume of the lesions was 32.9 cm^3 (range 7.8 cm^3 to 82.3 cm^3). For each patient three bone lesions were marked. Similarly, three lymph node and other (liver and prostate) lesions were delineated where applicable. For final analysis a mean value of every included parameter was determined.

2.2.4 Analysis of tumor textural heterogeneity

Tumor textural heterogeneity was assessed by extraction of local and global textural features from uptake histogram analysis and normalized gray-level co-occurrence matrix (NGLCM) respectively (Dong et al., 2016). The selected heterogeneity parameters were COV, entropy, homogeneity, contrast and size variation (Table 3). The selected parameters have been used widely in numerous PET studies and showed a statistically significant ability to depict the role of textural heterogeneity for analysis of tumor behavior (Dong et al., 2016; Eary et al., 2008; Cheng et al., 2013; Tixier et al., 2011; Pyka et al., 2015; Bundschuh et al., 2014; Divrik et al., 2012; Dong et al., 2015). SUV histogram analysis was used to calculate coefficient of variation (COV) (Chicklore et al., 2013; Tixier et al., 2012). Rest of the parameters, entropy, homogeneity, contrast and size variation were calculated from NGLCM contained three dimensional gray-level information (Chicklore et al., 2013; Tixier et al., 2012). For comparison purpose SUV as a conventional PET parameter was also analyzed.

2.2.5 Treatment response

After the baseline scan all patients underwent ^{177}Lu-PSMA therapy. The decision for ^{177}Lu-PSMA radioligand therapy was made by the local interdisciplinary tumor board at each therapy center. The protocol followed for therapy has already been explained in detail by rhaber et all (Rahbar et al., 2017). The parameters used to assess the response to ^{177}Lu-PSMA therapy were pre and post therapy changes in levels of PSA (prostate specific antigen), serum and bone alkaline phosphate and Eastern Cooperative Oncology Group (ECOG) criterion. Time difference between pre and post therapy levels was 7.1 weeks (average 6-8 weeks).

Parameter	Order	Description
COV	1st	A normalized measure of dispersion of a frequency distribution (standard deviation divided by the mean value of the activity concentration in the tumor volume).
Entropy	2nd	Measures randomness of distribution, e.g. a homogenous matrix demonstrates low entropy.
Homogeneity	2nd	A measure for continuous areas of same or similar voxel values in an image or voxel of interest (VOI).
Contrast	2nd	A measure of local variations present in the image. A high contrast value indicates a high degree of local variation.
Size Variation	3rd	Measures the difference of the grey value when going to the next voxel. It is high when the intensity changes very often between single voxels.

Table 3: Overview of textural heterogeneity parameters

2.2.6 Statistical Analysis

The statistical analysis was performed using SPSS (version 22, IBM). To evaluate the correlation between conventional and textural heterogeneity parameters and changes in pre and post therapy clinical parameters Spearman correlation was used. Statistical tests were conducted at a two-sided level of significance as $p < 0.05$

Receiver-operating-characteristics (ROC) analysis was also performed using MedCalc software (version 12.3.0.0; MedCalc). ROC analysis was performed to estimate the optimal cutoff value of the correlating parameters for response assessment. For this purpose, the Youden index was used to maximize the sum of sensitivity and specificity (Youden, 1950). The area under the curve (AUC) was calculated for each parameter using the nonparametric method developed by Hanley and McNeil (Hanley and McNeil, 1982)

representing the overall predictive or prognostic performance. For AUCs, exact binominal confidence intervals were calculated (95% confidence level), indicating the statistical significance of predictive capability if the critical value of 0.5 is not included.

2.3 Role of tumor textural heterogeneity in ^{68}Ga-PSMA PET-CT for therapy response assessment and prognosis in prostate cancer patients

2.3.1 Patient selection

50 patients with histologically proven prostate cancer were retrospectively included in this study. All patients were planned to undergo ^{177}Lu-PSMA-617 (abbreviated as ^{177}Lu-PSMA in this study) radioligand therapy. Clinical data was collected from November 2015 to April 2017. Average age of patients was 70.3 years.

Characteristic	Data
Age	70.3 years (51-88years)
Site of metastasis:	
Bone	50 (100%)
Lymph node	22 (44 %)
Other (liver, prostate)	7 (14 %)
Previous therapy of mCRPC:	
Androgen deprivation therapy	50 (100%)
Chemotherapy	26 (52.0%)
^{223}Ra	09 (18 %)
EBRT to bone	18 (36 %)

Table 4: Patient characteristics

Inclusion criteria for this retrospective analysis were progressive metastatic castration-resistant prostate cancer (mCRPC) patients. Patients experienced progression under next-generation androgen-deprivation therapy (e.g., abiraterone, enzalutamide) or first- or second-line chemotherapy (e.g., docetaxel, cabazitaxel) or were not eligible for chemotherapy. All patients eligible for ^{223}Ra received this treatment before undergoing ^{177}Lu-PSMA-617 radioligand therapy. 26 patients had prior chemotherapy. 09 patients had been treated previously with ^{223}Ra, while 18 patients had previous EBRT. All patients were refractory to hormone therapy.

2.3.2 ^{68}Ga-PSMA Scan:

Three ^{68}Ga-PSMA-617 (abbreviated in this study as ^{68}Ga-PSMA) PET scans were performed for every patient. Each patient underwent a baseline ^{68}Ga-PSMA scan before therapy with ^{177}Lu-PSMA termed as the pre-therapy scan. After the baseline scan patients underwent first ^{177}Lu-PSMA therapy. Renal function of every patient was analyzed prior to therapy with ^{99m}TC- MAG3 renal scintigraphy. A post therapy ^{68}Ga-PSMA scan was performed 6-8 weeks after the first therapy (average 7.6 weeks). This scan was termed as mid-therapy scan. After the mid-therapy scan two more PSMA therapies were given to every patient with an interval of 6-10 weeks (average 7.4 weeks). After completion of three therapies another ^{68}Ga-PSMA scan was performed labeled as post-therapy scan.

Data were acquired with a Biograph Sensation 2 PET-computer tomography (PET-CT) scanner (Siemens Medical Solutions). The axial and transverse fields of view were 16.2 and 58.5cm respectively. The transverse resolution of the scanner was about 6.5mm, whereas the axial resolution was 6.0mm, both at a radius of 10mm. The computer tomography (CT) component was a 2-slice spiral CT scanner. About 73 minutes (range 50-90 minutes) after the intravenous injection of approximately 131.3 MBq (range 98.8 to 174.8 MBq) of ^{68}Ga-PSMA, the patient was placed in the scanner. Low dose CT from the head to mid-thighs was performed followed by the PET scan of the same area in 6-7 bed positions, each for 3-4 minutes depending on the body weight of the patient. The CT data were

reconstructed in 512 x 512 pixel matrices. PET data was reconstructed into 128 x 128 matrices in axial, coronal and sagittal planes using the iterative attenuation-weighted ordered subset algorithm implemented by the manufacturer using 4 iterations and 16 subsets. Attenuation and scatter correction was performed using the CT data. Final voxel size was 5.3mm x 5.3mm x 5mm. All patients gave written and informed consent to the imaging procedure. All patient record and information was anonymized before analysis. Same protocol was followed for all three scan performed per patient.

2.3.3 PET Data Analysis

Image data were transferred to an Interview Fusion Workstation (Mediso Medical Imaging System, Budapest, Hungary). Firstly, co-registration between PET and CT images was performed. Tumor volume was manually delineated on PET images. Tumor volume was manually delineated on PET images (Figure 1) with a standard uptake value (SUV) threshold (Fendler, 2017; Mathieu, 2015).). All the 50 patients had bone metastasis. Twenty two patients had lymph node metastasis along with bone metastasis. Seven patients had additional liver and/or prostate lesions. Three VOIs each for bone and lymph node lesions were delineated. Other lesions were also delineated if present in liver and prostate. Parameters to be evaluated were measured in these VOIs. A total of 260 VOIs were delineated. Mean volume of the lesions was 36.4 cm^3 (range 8.2 cm^3 to 82.3 cm^3). For each patient three bone lesions were marked. Similarly, three lymph node and other (liver and prostate) lesions were delineated where applicable. For final analysis a mean value of every included parameter was determined.

2.3.4 Analysis of tumor textural heterogeneity

Tumor textural heterogeneity was assessed by extraction of local and global textural features from uptake histogram analysis and normalized gray-level co-occurrence matrix (NGLCM) respectively (Dong et al., 2016). The selected heterogeneity parameters were COV, entropy, homogeneity, contrast and intensity variation (Table 5).

Parameter	Order	Description
COV	1st	A normalized measure of dispersion of a frequency distribution (standard deviation divided by the mean value of the activity concentration in the tumor volume).
Entropy	2nd	Measures randomness of distribution, e.g. a homogenous matrix demonstrates low entropy.
Homogeneity	2nd	A measure for continuous areas of same or similar voxel values in an image or voxel of interest (VOI).
Contrast	2nd	A measure of local variations present in the image. A high contrast value indicates a high degree of local variation.
Intensity Variation	2nd	The intensity variation describes the variation of the intensity of different substructures.

Table 5: Overview of textural parameters

The selected parameters have been used widely in numerous PET studies and showed a statistically significant ability to depict the role of textural heterogeneity for analysis of tumor behavior (Dong et al., 2016; Eary et al., 2008; Cheng et al., 2013; Tixier et al., 2011; Pyka et al., 2015; Bundschuh et al., 2014; Divrik et al., 2012; Dong et al., 2015). SUV histogram analysis was used to calculate coefficient of variation (COV) (Chicklore et al., 2013; Tixier et al., 2012). Rest of the parameters, entropy, homogeneity, contrast and intensity variation were calculated from NGLCM contained three dimensional gray-level information (Chicklore et al., 2013; Tixier et al., 2012). Intensity variation was also included due to its close approximation with entropy (measure of randomness of intensity values in an image (Alobaidli et al., 2014)) which is usually the determining feature in numerous studies. For comparison purpose SUV as a conventional PET parameter was also analyzed.

2.3.5 Treatment response

Each patient underwent three ^{177}Lu-PSMA therapies and three ^{68}Ga-PSMA scans. The decision for ^{177}Lu-PSMA radioligand therapy was made by the local interdisciplinary tumor board at each therapy center. The protocol followed for therapy has already been explained in detail by rhaber et all (Rahbar et al., 2017). The parameters used to assess the response to ^{177}Lu-PSMA therapy for each therapy were pre and post therapy changes in levels of PSA (prostate specific antigen), serum and bone alkaline phosphate and Eastern Cooperative Oncology Group (ECOG) criterion. Data were collected for consecutive three ^{177}Lu-PSMA therapies. For calculation of overall survival, the time between the first PET/CT examination and the date of death was used.

2.3.6 Statistical Analysis

Receiver-operating-characteristics (ROC) analysis was performed using MedCalc software (version 12.3.0.0; MedCalc). ROC analysis was performed to estimate the optimal cutoff value of the correlating parameters for response assessment. For this purpose, the Youden index was used to maximize the sum of sensitivity and specificity (Youden, 1950). The area under the curve (AUC) was calculated for each parameter using the nonparametric method developed by Hanley and McNeil (Hanley and McNeil, 1982) representing the overall predictive or prognostic performance. For AUCs, exact binominal confidence intervals were calculated (95% confidence level), indicating the statistical significance of predictive capability if the critical value of 0.5 is not included.

The relationship of the investigated parameters with overall survival, was analyzed using Kaplan–Meier plots. Kaplan–Meier analysis was performed using thresholds previously established by ROC analysis. Differences between Kaplan–Meier curves were evaluated using nonparametric log-rank tests, considering differences with a P value smaller than 0.05 to be significant.

3. Results

The study showed some very good results. As in previous sections the results will also be divided into three parts.

3.1 Role of textural heterogeneity parameters in diagnosis of pseudoprogression in high grade gliomas

3.1.1 Patient characteristics

The study population comprised 14 patients (Table 5) with histologically proven high-grade glioma. A methylated MGMT promoter was found in 12 and a non-methylated MGMT promoter in 2 patients. All patients underwent radiotherapy before PET investigation, either concomitant with chemotherapy or separated. Nine patients included in the study underwent FET-PET investigation while during first-line treatment whereas five patients after relapse had occurred.

3.1.2 Diagnosis of true tumor progression versus pseudoprogression

Four of fourteen patients had confirmed PSP. Ten patients were regarded as having unequivocal progression (Table 6). All patients diagnosed with PSP had a methylated MGMT promoter whereas the MGMT promotor was methylated in 80% (8 of 10) in patients with true tumor progression.

3.1.3 Identification of FET-PET-based subtypes

As shown in Figure 5a, the consensus matrix displays a well-defined 3-block structure for k=3, corresponding to three distinct cluster groups. The cumulative distribution function (CDF) curve, which plots consensus distributions for each k, approaches at k=3 the ideal step function and its shape hardly changes as k is increased past 3 (Figure 5b). The difference between two CDF curves (at k and k+1) is summarized by measuring the area

Patient No.	Cluster	Sex	Age at Dx [year]	Histologic Dx	MGMT methylated?	Line of therapy	Treatment regimen until PET investigation	Concomitant dexamethasone treatment?	Wks from last Rx	Follow-up MRI + Clin.	Follow-up Time [months]	PFS [months]	OS [months]
1	1	m	29	AA	yes	1	**P:** B,RT+TMZ	no	7	Stable	27.2	>26.7	>27.2
3	1	m	45	GBM*	yes	2	**P:** B,TMZ; **1R:** R,RT,PC	yes	16	prog.	16.4	8.4	16.4
4	1	f	40	AOA	yes	4	**P:** pR; **1R:** TMZ; **2R:** TMZ; **3R:** pR,RT, CCNU	no	34	prog.	126.4	>26.1	>126.4
10	1	m	43	GBM*	no	1	**P:** pR,RT,PC	no	37	prog.	24.1	8.0	24.1
12	1	m	70	GBM	yes	2	**P:** pR,RT+TMZ,TMZ; **1R:** R,TMZ	no	139	prog.	45.1	4.1	45.1
14	1	f	68	GBM	yes	1	**P:** cR,RT+TMZ,TMZ	yes	10	prog.	23.4	>22.1	>23.4
5	2	f	49	GBM	no	1	**P:** pR,RT+TMZ,TMZ	no	52	prog.	34.1	4.6	34.1
6	2	m	61	GBM	yes	2	**P:** cR,RT+TMZ,TMZ; **1R:** R,RT,CCNU/TMZ	no	25	prog.	23.5	>13.3	>23.5
8	2	m	60	GBM	yes	1	**P:** cR,RT+TMZ,TMZ	no	33	prog.	11.3	2.2	11.3
13	2	m	54	GBM	yes	1	**P:** pR,RT+TMZ	no	4	prog.	10.0	6.0	10.0
2	3	m	59	GBM	yes	1	**P:** R,RT+TMZ/CCNU, TMZ/CCNU	no	95	stable	44.3	>21.7	>44.3
7	3	f	47	AA	yes	1	**P:** B,RT+TMZ,TMZ	no	25	stable	27.5	16.7	27.5
9	3	f	66	GBM	yes	1	**P:** cR,RT+TMZ,TMZ	no	48	prog.	21.7	5.1	21.7
11	3	m	50	GBM	yes	2	**P:** cR,RT+TMZ,TMZ; **1R:**R,RT+CCNU/TMZ, CCNU/TMZ	no	41	stable	49.3	13.9	49.3

Table 6: Patient Characteristics

Abbreviations: AA, anaplastic astrocytoma; Clin., clinical follow-up.; cR, complete resection; Dx, diagnosis; Follow-up Time, time from diagnosis to last follow-up; GBM*, secondary glioblastoma; GBM, glioblastoma; CCNU, lomustine; MGMT, O-6-methylguanine-DNA methyltransferase; stable, no progression; nyr, not yet reached; PET, positron emission tomography; pR, partial resection; prog., progression; R, resection of unknown extent; RT, radiotherapy; RT+CCNU/TMZ, combined radiotherapy and chemotherapy with temozolomide and lomustine; RT+TMZ, combined radiotherapy and chemotherapy with temozolomide; TMZ, temozolomide; wk, weeks; y, years; B, biopsy; OS, overall survival; PC, procarbazine and lomustine; PFS, progression-free survival; m, months, # Line of therapy while under PET investigation; >, indicates censored values

under the CDF curves for k=2 through 7 and shown in Figure 5c. As k is increased, the area under the CDF curve stays approximately the same until k=3 and drops off significantly beyond that value. Any further increase in k does not come along with a corresponding marked increase in the CDF area, thus further supporting the choice of an optimal k=3.

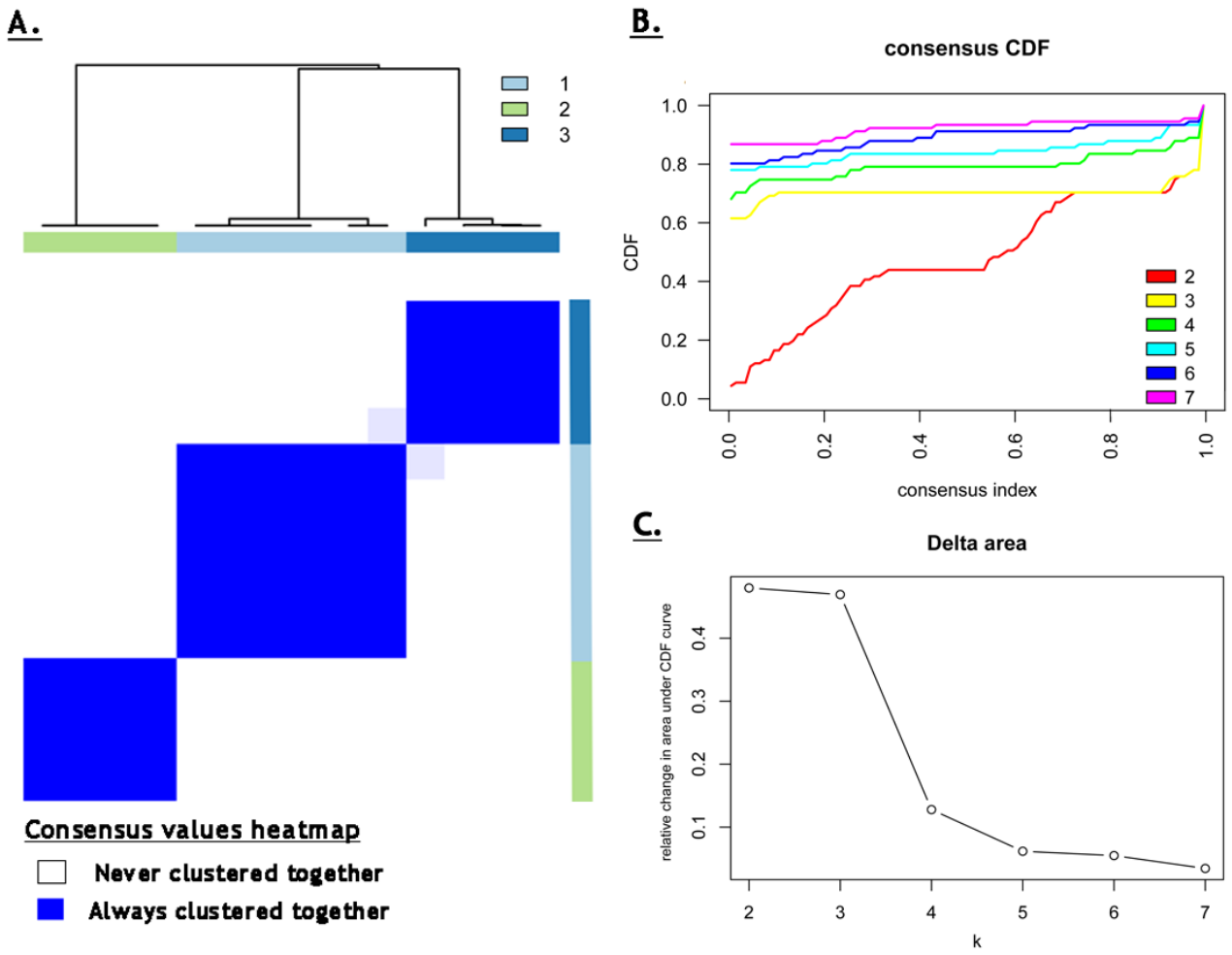

ill 5: Consensus matrix heat map

This result was confirmed by using the recently published PAC method, which was shown to be more accurate in determining the right number of k, where PAC was lowest at k=3, reflecting an optimal clustering with three groups. Of the 14 patients in our cluster cohort, six patients were assigned to cluster 1 (43%), and four patients (29%) each were assigned to cluster 2 and 3.

3.1.4 Assigning FET-PET features to each cluster

To identify FET-PET features associated with each cluster we used the nearest shrunken centroid method called predictive analysis of microarrays (PAM). Predictor discovery by PAM identified ten PET features out of 19 with at least one nonzero component. This implies that those selected features simultaneously distinguish all clusters from each other. Figure 6a shows a heatmap of all hierarchically clustered features corresponding to each cluster and Figure 6b shows the shrunken differences for the ten PET characteristics differentially regulated across the three clusters. Of those, 8 characteristics are textural features (Contrast, Entropy, Correlation, Size Var, Coarseness, Volume, COV, and Complexity) and two are recognized as conventional (TLG, Max). Notably, the upper 7 (figure 6b) of those 10 features provide the most distinct separation among clusters: Contrast, Volume, Entropy, TLG, Correlation, Size Variation, and Coarseness.

From the distribution of FET-PET features across clusters using PAM, it becomes evident that cluster 2 was particularly associated with high values of the textural characteristics Contrast and Entropy (Figure 6b). As increased values of both features have been tied to intratumoral tracer uptake heterogeneity, the cluster 2 phenotype was designated "high heterogeneity cluster". Except for the feature Coarseness, cluster 3 was largely associated with inverse loadings of FET-PET textural features as compared with cluster 2, most strikingly Entropy, Correlation and Size zone variability. With high intratumoral tracer uptake heterogeneity, Entropy and Correlation are known to be increased and Size-zone variability decreased. It was thus named "low heterogeneity cluster". Interestingly, TLG was also

comparably downregulated in this cluster. As opposed to cluster 2 and 3, cluster 1 had the least variability in features. Only the feature Correlation was considerably upregulated. As such, cluster 1 was defined as "intermediate cluster".

3.1.5 Pseudoprogression and cluster assignment

All of the patients assigned to cluster 2 (4 out of 4) and five out of six of cluster 1 were diagnosed with progression, whereas three of four patients with pseudoprogression fell into cluster 3 (Figure 6a).

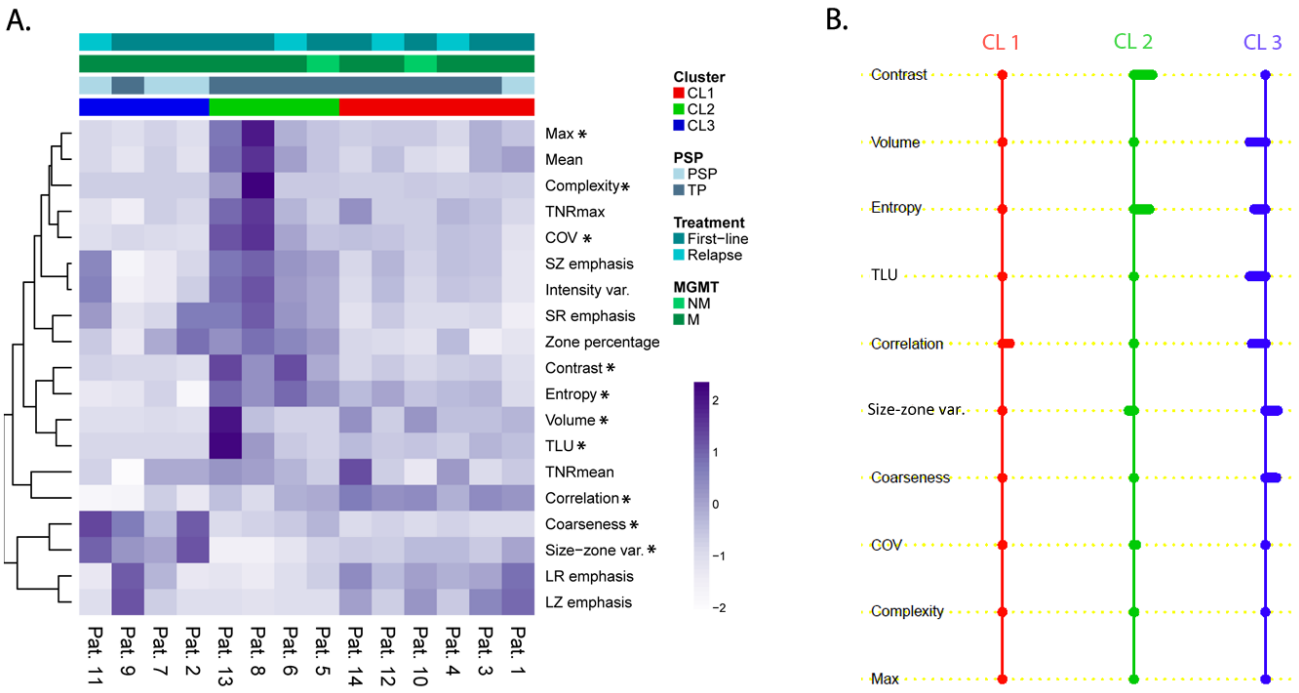

C.

	Cluster 3 vs remainder	TNRmax cutoff 2.1
Sensitivity (95% CI)	0.9 (0.54 - 0.99)	0.7 (0.42 - 0.90)
Specificity (95% CI)	0.75 (0.22 - 0.99)	1.0 (0.35 - 0.92)
PPV (95% CI)	0.9 (0.54 - 0.99)	1.0 (0.56 - 1.00)
NPV (95% CI)	0.75 (0.22 - 0.99)	0.57 (0.20 - 0.88)
p-value (Fisher's exact)	0.041	0.070

ill 6: Cluster analysis

Usually, patients with suspected pseudoprogression and an increased TNRmax value (optimal cutoff of 2.1 in this study) were diagnosed with tumor progression. Figure 5c illustrates the explorative comparison of the diagnostic value in detecting true tumor progression of TNRmax with an assignment to cluster 3. Cluster 3 seems to be stronger associated with the detection of true progression (p=0.041) compared to increased TNRmax group (p=0.07). Cluster 3 provided a high sensitivity and specificity (90% and 75%, respectively) for detecting true progression with a negative predictive value (NPV) of 75%. TNRmax similarly provided high values for specificity and sensitivity (70% and 100%, resp ectively), yet, at the cost of a low NPV (57%).

3.1.6 Putative prognostic value of clusters

To investigate further each cluster phenotype, we calculated the progression-free survival (PFS) measured from the time of PET investigation to the date of following tumor progression based on RANO evaluation. As shown in Figure 7a, patients grouped to cluster 2 seem to have a lower median PFS (5.3 months vs. 14.6 months in cluster 1 and 15.3 months in cluster 3). When calculating median PFS using Kaplan-Meier method – accounting for censored values - cluster 2 remains the one with the lowest median PFS (4.6 months vs. 8.4 months in cluster 1 and 13.9 months in cluster 3). Figure 7b illustrates that this effect might not be explained by differentially distributed prognostic factors among clusters, given a balanced distribution of prognostic factors.

A.

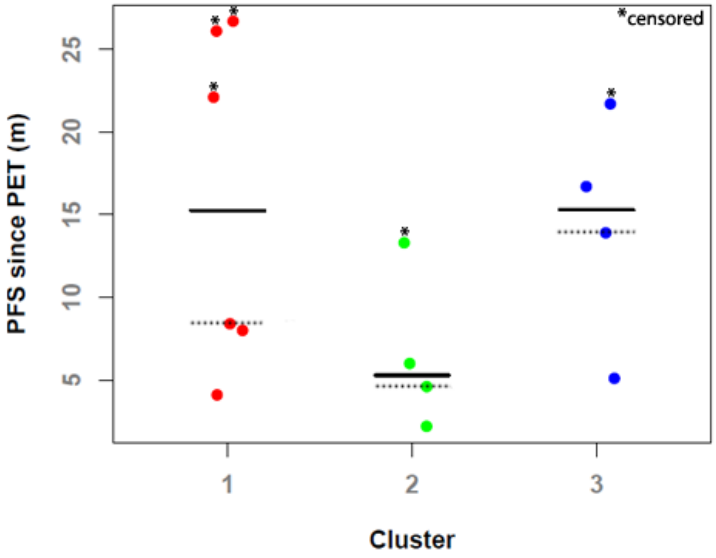

B.

	Cluster1 (n=6)	Cluster 2 (n=4)	Cluster 3 (n=4)	p-value
Age, mean (SD)	49 (16.3)	55 (8.7)	56 (5.6)	0.578 (k)
Sex, female, n (%)	2 (33.3)	2 (50)	1 (25)	0.752 (f)
Mean KPS, mean (SD)	83 (15.1)	88 (5.0)	90 (8.2)	0.849 (k)
MGMT, methylated, n (%)	5 (83)	4 (100)	3 (75)	0.586 (f)
Complete resection, n (%)	1 (20)	2 (50)	3 (75)	0.261 (f)

C.

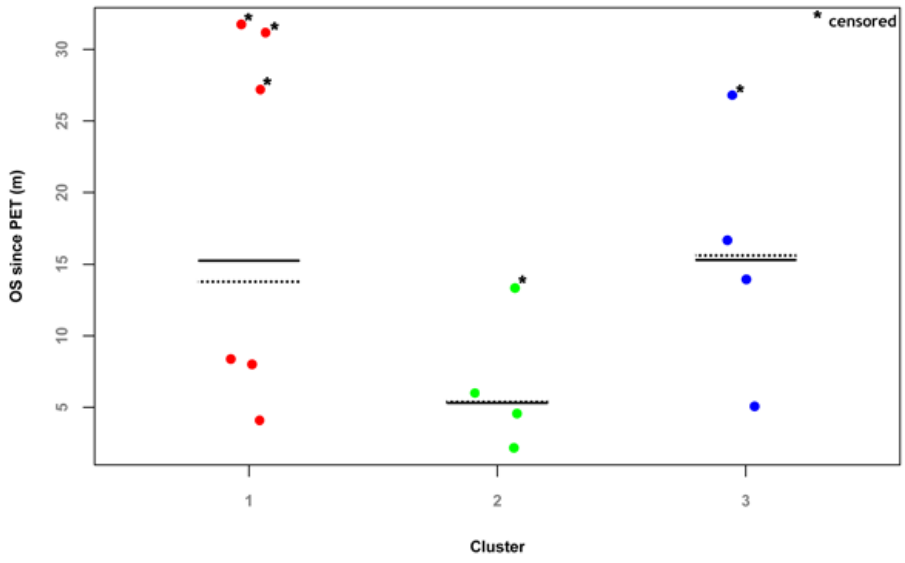

ill 7: Progression free survival analysis

3.2 Role of textural heterogeneity parameters in patient selection for ^{177}Lu-PSMA therapy

Seventy patients were evaluated in this study. Decrease in PSA level was observed in 42 patients (60%) and they were labeled as responders to therapy. Increase in PSA level was seen in 28 patients (40%) considered as non-responders (Figure 8(a)).

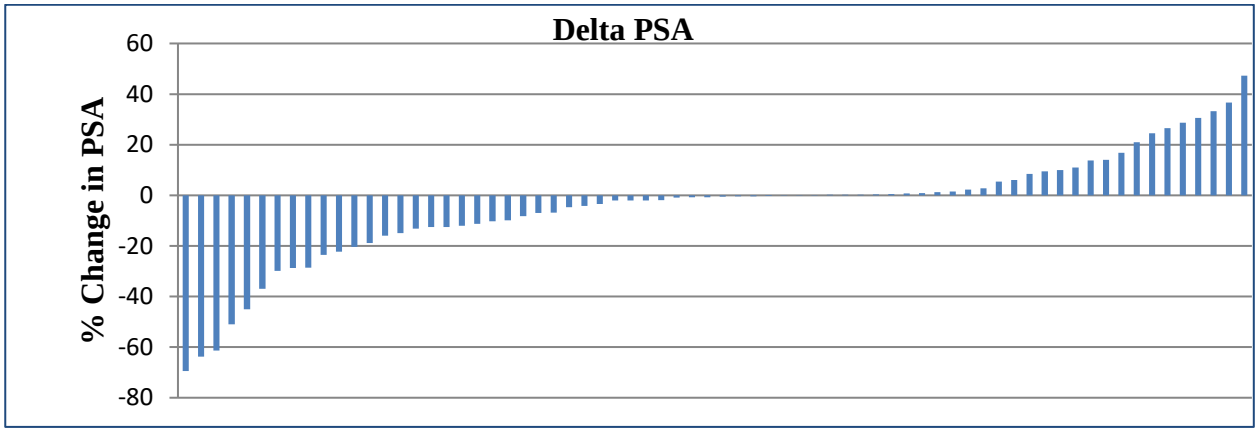

ill 8(a): Percentage change in PSA

41 patients (58%) showed response via decrease in serum alkaline phosphate level (Figure 8(b)) and 39 patients (55%) showed response by decrease in bone specific alkaline phosphate (Figure 8(c)). Among the responders 24 patients (34.2%) showed decrease in both PSA and alkaline phosphate levels at the same time while 22 patients (31.42%) showed decrease in PSA, alkaline phosphate and bone specific alkaline phosphate levels together. No change was observed in ECOG of any patient.

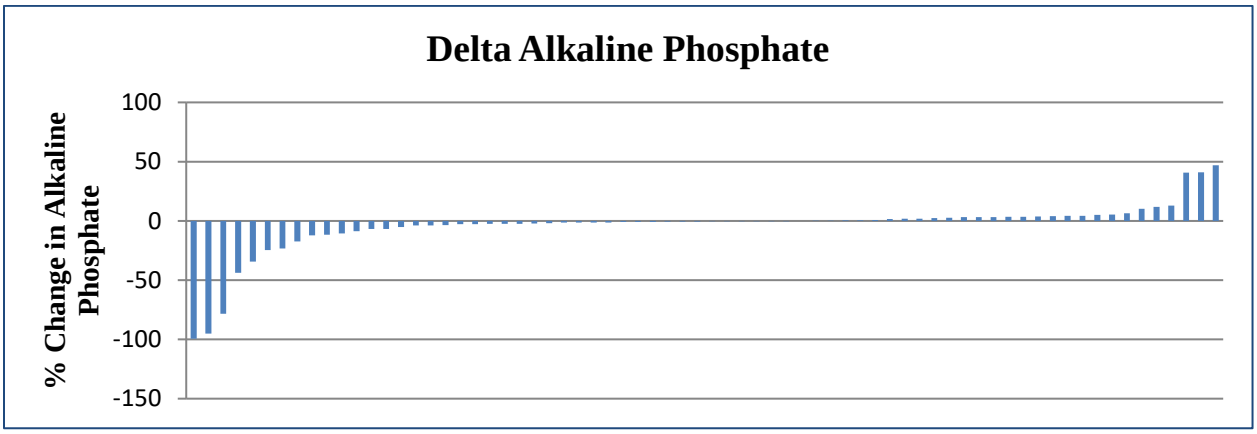

ill 8(b): Percentage change in Alkaline Phosphate

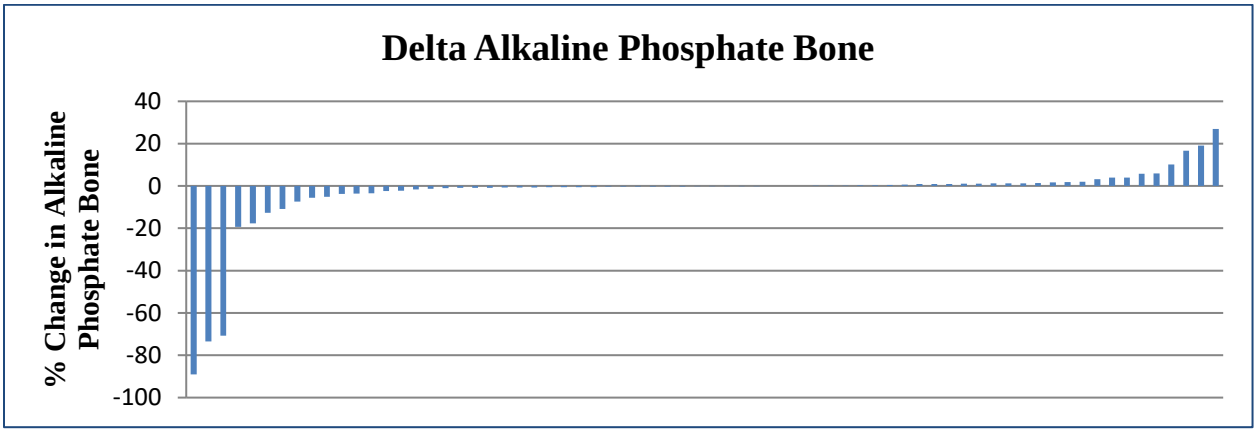

ill 8(c): Percentage change in Alkaline Phosphate Bone

Analysis of PET based heterogeneity parameters revealed that only two textural heterogeneity parameters entropy and homogeneity showed correlation with change in pre and post therapy PSA levels. PSA levels which showed correlation were derived from bone lesions. Lymph node and other lesions derived values did not show any correlation. Change in pre and post therapy values of serum alkaline phosphate, bone specific alkaline phosphate and individual patient ECOG status derived from all types of lesions remained uncorrelated. Similarly textural heterogeneity parameters other than entropy and homogeneity also remained uncorrelated. Actual values of correlating parameters as obtained through Spearman correlation are as under.

Entropy showed a negative correlation (r_s = -0.327 and p = 0.006) and homogeneity showed a positive correlation (r_s = 0.315 and p = 0.008) with change in pre and post therapy PSA levels (Figures 9 (a) and (b)).

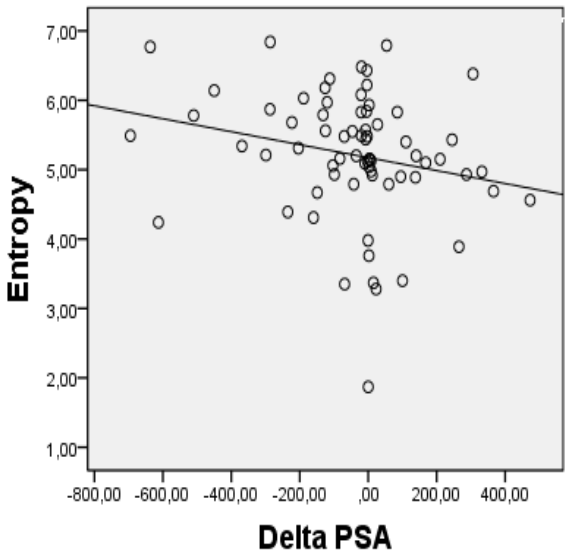

ill 9(a): Representation of negative correlation between absolute ∆PSA(ng/ml) and entropy of bone lesions (R^2 = 0.283)

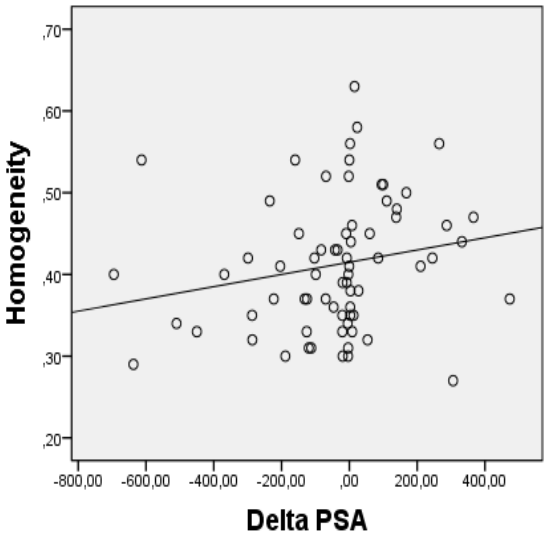

ill 9(b): Representation of positive correlation between absolute ∆PSA (ng/ml) and homogeneity of bone lesions (R^2 = 0.326)

It is essential to be taken into account that change in PSA levels was obtained as post therapy levels minus the pre therapy level (post therapy PSA – pre therapy PSA). A negative value of this equation meant that post therapy PSA was less than that of pre therapy and the case was considered as of a responder. So the resultant value of a responder was negative and vice versa. Hence, a negative correlation of entropy with this change (also represented with a negative value) meant that entropy and change in PSA levels was directly proportional to each other. Or in other words the responders showed a higher entropy value. Similarly, homogeneity showed a positive correlation and hence a negative proportionality with the change in PSA levels signifying that the responders had a lower homogeneity.

Below is a table (Table 7) summarizing the positive results i.e. obtained by correlating positive textural heterogeneity parameters obtained from bone lesions with

change in pre and post therapy PSA levels. Rest of the parameters are also given for comparison. It can be also seen that SUV values also did not positively correlate.

PET Parameter (Bone Lesions)	Correlating Clinical Parameter	Spearman Coefficient	p-value
Entropy	ΔPSA	0.327	0.006
Homogeneity	ΔPSA	-0.315	0.008
COV	ΔPSA	0.113	0.516
Contrast	ΔPSA	0.257	0.136
Size Variation	ΔPSA	-0.309	0.071
SUV(mean)	ΔPSA	0.168	0.333

Table 7: Correlation of bone lesion derived PET parameters with change in PSA level

The ROC analysis also showed that entropy and homogeneity are statistically significant ($p < 0.05$) for predictive ability. Further results of ROC analysis are summarized in the table below (Table 8).

Parameter	AUC (Area under curve)	95% Confidence Interval	Cut-off Value (based on Youden Index)
Entropy	0.695	0.573 to 0.799	>5.15
Homogeneity	0.683	0.561 to 0.789	≤0.43

Table 8: Results of ROC Analysis for Predictive Value of Pre therapeutic PET- CT

Sensitivity and specificity was also assessed for both parameters through ROC (Figure 10(a)and (b)) and these values were used to find out positive and negative predictive values (Table 9).

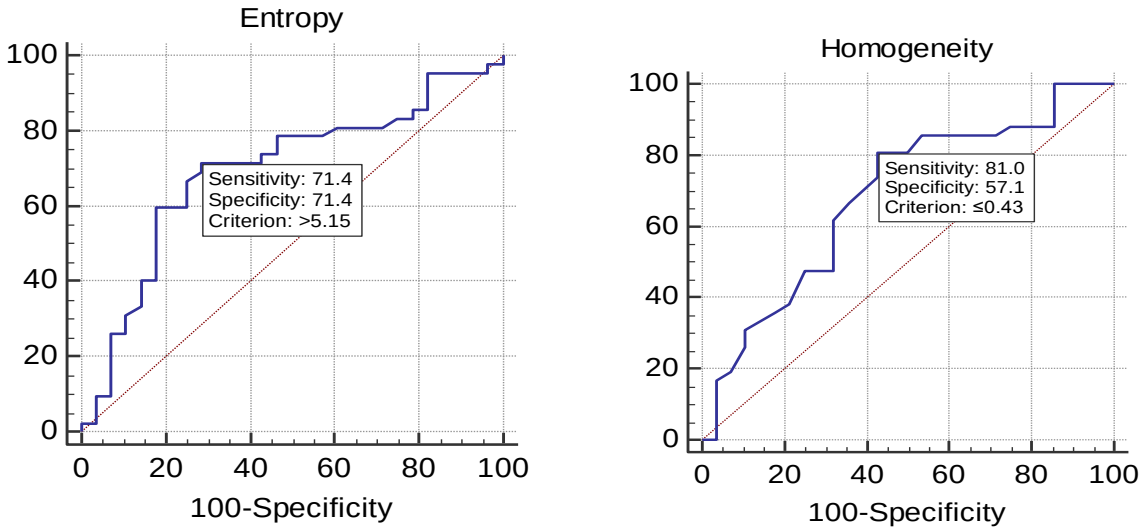

Ill 10 (a) and (b): Showing results of ROC analysis

Parameter	Sensitivity	Specificity	Positive Predictive Value	Negative Predictive Value
Entropy	71.4 %	71.4 %	62.50 %	78.95 %
Homogeneity	81 %	57.1 %	66.67 %	73.91 %

Table 9: Outcomes of positive parameters

For the above mentioned parameters, the combined sensitivity of entropy and homogeneity for predicting outcome was 57.83% and the combined specificity was 87.74%.

3.3 Role of Tumor Textural Heterogeneity in ^{68}Ga-PSMA PET-CT for Therapy Response Assessment and Prognosis in Prostate Cancer Patients

Fifty patients were evaluated in this study. Decrease in PSA level was observed in 31 patients (62%) and they were labeled as responders to therapy. Increase in PSA level was seen in 19 patients (38%) considered as non-responders.

29 patients (58%) showed response via decrease in serum alkaline phosphate level and 27 patients (54%) showed response by decrease in bone specific alkaline phosphate. No change was observed in ECOG of any patient till the completion of third therapy.

Analysis of heterogeneity parameters in the bone lesions showed that three parameters had statistically significant predictive capability. These three parameters were entropy, homogeneity and intensity variation. The significance of parameters was ascertained through independent T-test and ROC analysis. Conventional parameters SUV mean and max did not show any statistical significance. Similarly, lesions in lymph nodes and other organs (liver, prostate) did not show any statistical significance.

The ROC analysis was performed for changes in measured for pretherapeutic PET-CT, mid-therapy PET-CT and post-therapy PET-CT examinations. The results of these measurements are presented in Table 10.

Parameter	AUC	95% Confidence Interval	p-value (0.05)
Pre-Therapy			
Entropy	0.725	0.546-0.864	0.018
Homogeneity	0.603	0.421-0.766	0.030
Intensity Variation	0.659	0.477-0.812	0.05
Mid-Therapy			
Entropy	0.687	0.505-0.834	0.042
Homogeneity	0.679	0.498-0.828	0.057
Intensity Variation	0.681	0.500-0.830	0.06
Post-Therapy			
Entropy	0.712	0.532-0.854	0.001
Homogeneity	0.755	0.577-0.885	0.002
Intensity Variation	0.716	0.536-0.857	0.038

Table 10: Results of ROC analysis

In the pretherapeutic scans entropy had the highest AUC and the lesions with higher entropy and intensity variation and low homogeneity showed better response to the first therapy. While in the post-therapy scans homogeneity showed the highest AUC and the lesions with higher homogeneity and lower entropy showed better response to therapy. This is in contrast with the pretherapeutic scan results. The lesions having persistently higher entropy and size variation or lower homogeneity showed poor prognosis after three therapies. We found that in pre-therapy scans a higher entropy and size variation and lesser homogeneity was good selection criterion for patients but after subsequent therapies (three in our study) lower entropy and size variation and higher homogeneity were indicators of good outcome.

Entropy:

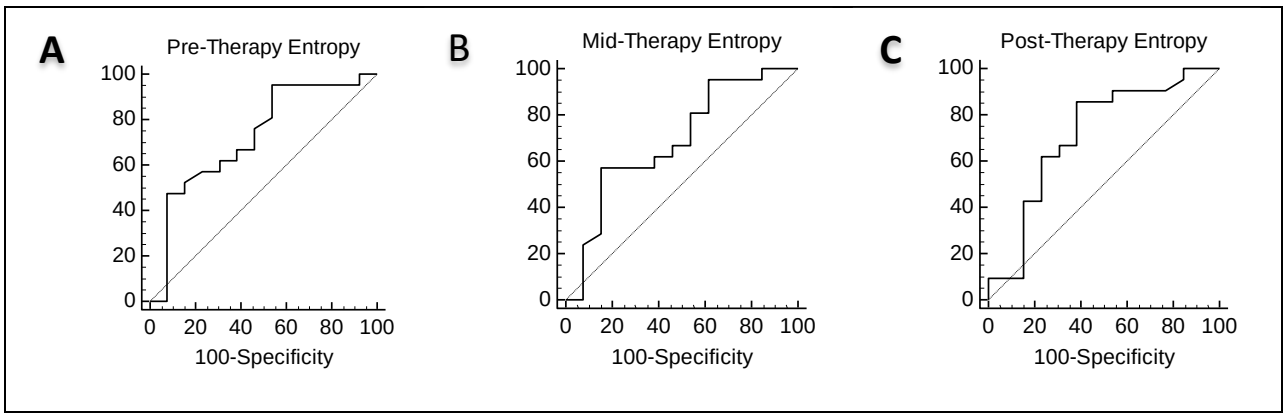

Homogeneity:

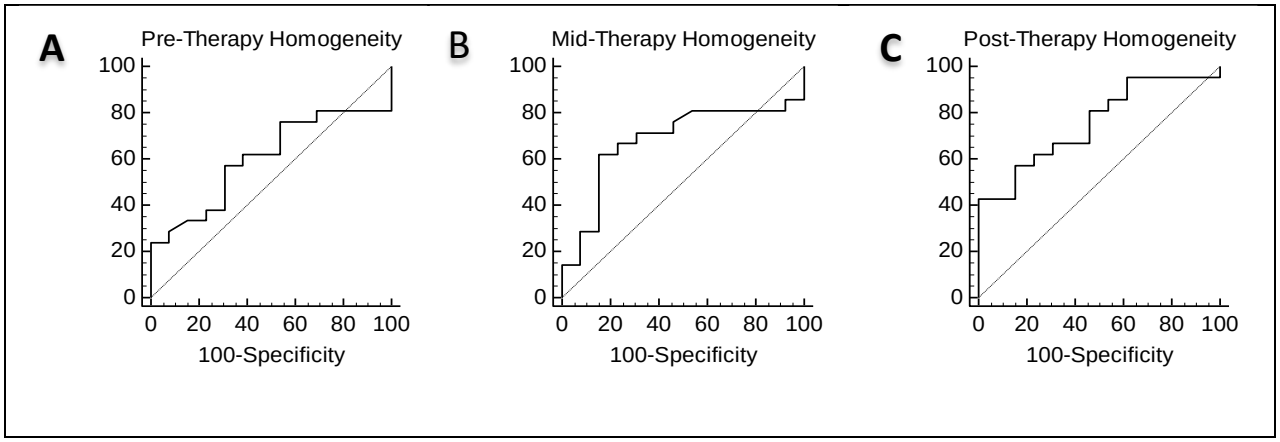

Intensity Variation:

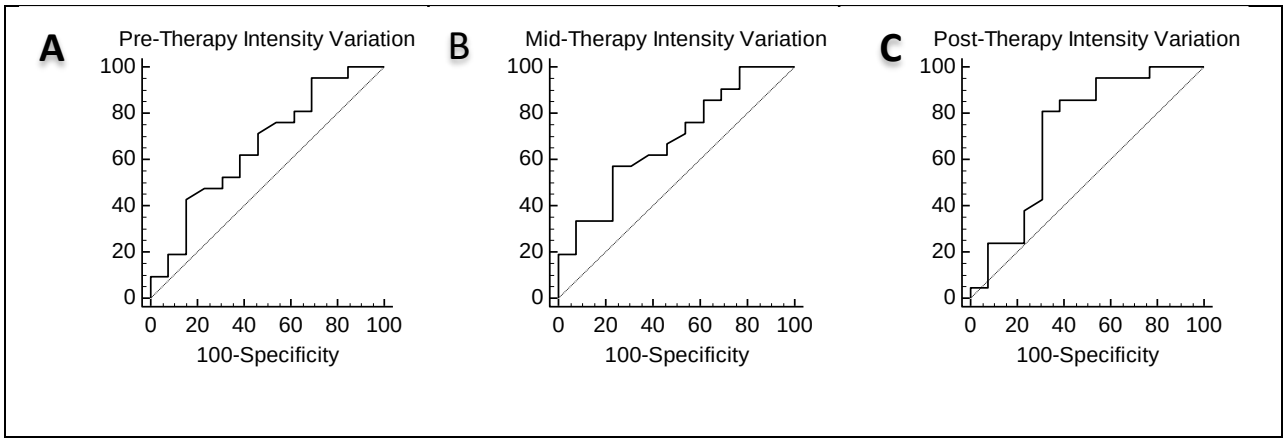

ill 11: ROC analysis

No statistically significant correlation was found between the textural parameters and lesion volume. In addition, the positive outcomes were obtained only for bone lesions and only those in comparison to change in serum PSA levels. The lymph node lesions showed no statistical significance and similarly, correlation with alkaline phosphate, bone alkaline phosphate and ECOG criterion was also not statistically significant.

The sensitivity and specificity of the parameters was also calculated for predicting outcome with change in PSA as standard. The results are showed in following table.

Parameter	Sensitivity	Specificity
Pre-Therapy		
Entropy	79.2 %	46.1 %
Homogeneity	69.4 %	57.1 %
Intensity Variation	42.8 %	84.6 %
Mid-Therapy		
Entropy	57.1 %	84.6 %
Homogeneity	61.9 %	84.6 %
Intensity Variation	57.1 %	76.9 %
Post-Therapy		
Entropy	85.7 %	61.5 %
Homogeneity	42.8 %	100 %
Intensity Variation	80.9 %	69.2 %

Table 11: Sensitivity and specificity of parameters

During a mean follow-up of 900 days, progressive disease was found in 19 patients. Increased PSA levels were detected in all patients with progression. Fifteen patients of the study group died within the follow up time, on average 510 days after the first PET-CT examination (range, 187 - 776 days).

Entropy:

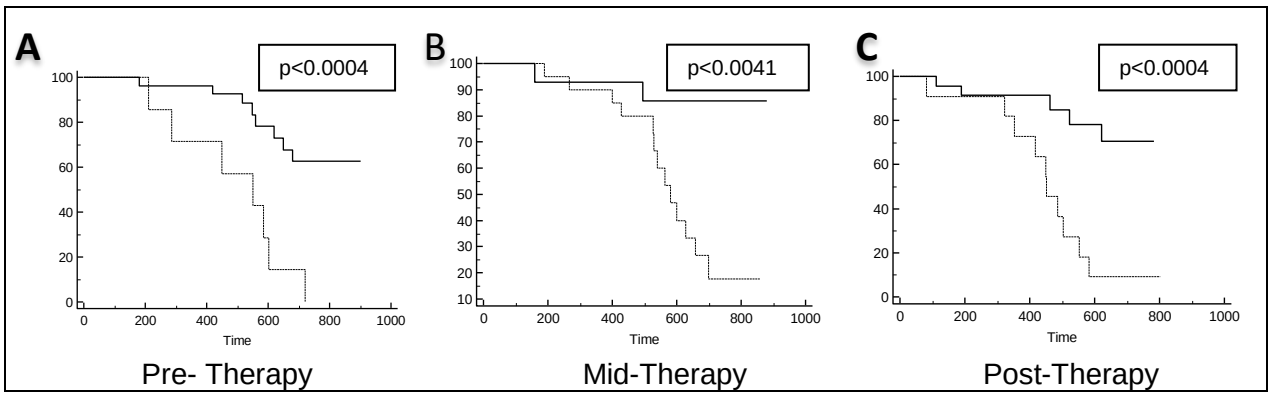

Homogeneity:

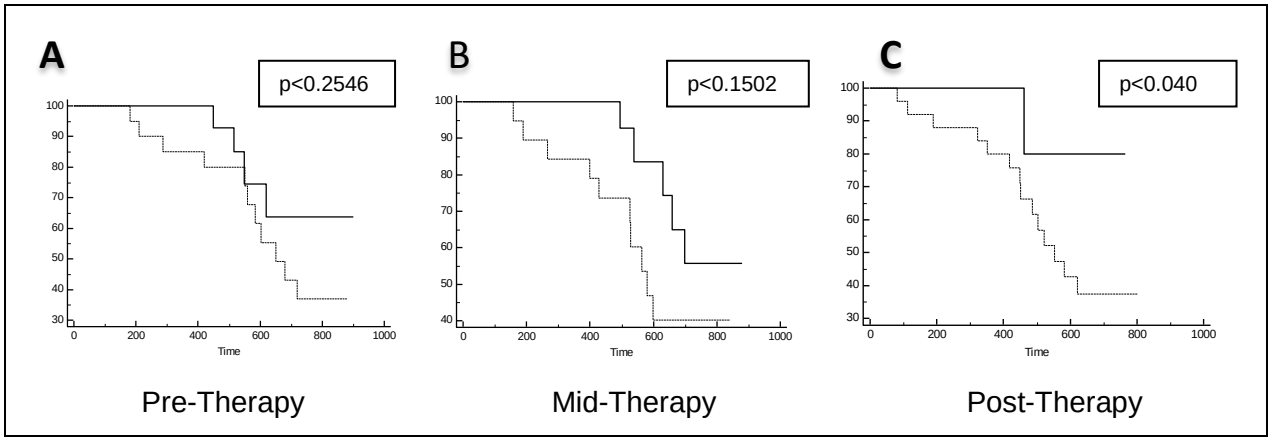

Intensity Variation:

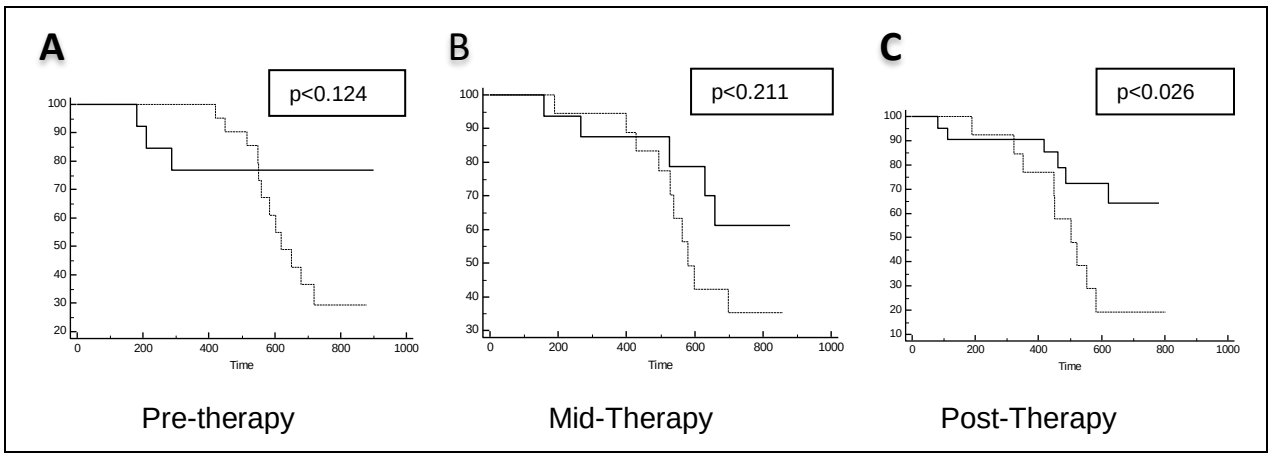

ill 12 : Kaplan-Meier analysis

Kaplan–Meier analysis showed all three parameters to have a statistically significant prognostic capability for overall survival analysis. The corresponding Kaplan–Meier plots are shown in figure 3.

p-values indicating a prognostic capability are shown in the graphs. It can be seen that entropy shows the most statistically significant capability to predict overall survival from pre, mid and post therapy scans. However, homogeneity and intensity variation were able to predict survival only from the data acquired via post-therapy scans. We also calculated combined sensitivity and specificity for all three predictors from the values obtained by post therapy scan.

Combined sensitivity of entropy and intensity variation for predicting outcome was 69.3 and the combined specificity was 88.1

Combined sensitivity of entropy and homogeneity for predicting outcome was 91.9 and the combined specificity was 61.5

The median overall survival for entropy which proved to be the best indicator in analysis is shown in the table below.

Time Point	Parameter	Mean Overall Survival
Pre-therapy	Entropy ≥ 5.06	722 days
	Entropy < 5.06	376 days
Mid-therapy	Entropy ≥ 5.87	701 days
	Entropy < 5.87	436 days
Post-therapy	Entropy ≤ 5.38	624 days
	Entropy > 5.38	254 days

To investigate whether the tumor heterogeneity or the change in heterogeneity during therapy depended on the lesion size or the change in lesion size, we performed a Pearson correlation analysis of positive parameters for heterogeneity with the lesion volume. No correlation was found between lesion volume and textural heterogeneity parameters in all parts of the study.

4. Discussion

In this study, we analyzed the capability of textural markers to assess heterogeneity in PET to predict therapy response and outcome in patients. Assessment of tumor heterogeneity is becoming an effective tool for analysis of tumor and therapy behaviors. Most important is this analysis can be performed on in depth image analysis and is much easier and efficient than the invasive methods. Instead of being only a qualitative analysis, analysis of textural heterogeneity helps in extracting quantitative information from the images as well (Aerts et al., 2014). Textural analysis is the measure of spatial variation at different levels of a tumor like imaging, gross morphology, cellular and genetic level. It is known that multiple subclonal populations coexist within tumors, reflecting extensive intratumoral somatic evolution (Yachida et al., 2010; Gerlinger et al., 2012). This heterogeneity is a clear barrier to the goal of personalized therapy based on molecular biopsy-based assays, as the identified mutations and gene-expression does not always represent the entire population of tumor cells (Gerlinger and Swanton, 2010; Kern, 2012).

Genetic variations in tumors can be related to a mutator phenotype that generates new clones, some of which expand into large populations (Nowell, 1976). However, although identification of genotypes is of substantial interest, it is insufficient for complete characterization of tumor dynamics because evolution is governed by the interactions of environmental selection forces with the phenotypic, not genotypic, properties of populations as shown, for example, by evolutionary convergence to identical phenotypes among cave fish even when they are from different species (Greaves and Maley, 2012; Vincent and Brown, 2005; Gatenby and Gilles, 2008). This connection between tissue selection forces and cellular properties has the potential to provide a strong bridge between medical imaging and the cellular and molecular properties of cancers (Gatenby et al., 2013). Thus it can be said that continued tumor variation/evolution can be attributed to tumoral heterogeneity at genetic level. Evolution within tumors is governed by Darwinian dynamics,

with identifiable environmental selection forces that interact with phenotypic (not genotypic) properties of tumor cells in a predictable and reproducible manner; clinical imaging is uniquely suited to measure temporal and spatial heterogeneity within tumors that is both a cause and a consequence of this evolution (Gatenby et al., 2013). Analysis of this spatial variation by computer generated algorithms working on superimposition of multiple sequined images can lead to individual specific evaluation of intratumoral variation and can thus form a basic factor for personalized therapy.

PET being a multimodal modality for imaging, giving both the anatomical and physiological information is gaining momentum for analysis of tumor textural heterogeneity. When considering the PET component, it refers to radiotracer uptake spatial distribution, which may reflect, depending on the radiotracer used, the combination of underlying biological processes such as metabolism, hypoxia, cellular proliferation, vascularization and necrosis (Willaime et al., 2013; Weber et al., 2000). Regarding the low-dose CT component of PET-CT, usually without contrast enhancement, heterogeneity refers to the variability in tissue density, which may result from spatially varying vascularization, necrosis or cellularity, as well as the proportions of fat, air and water (Aerts, 2014). With other modalities such as contrast-enhanced CT, as well as in MRI using various sequences (for example, T1, T2, FLAIR, DCE-MRI), heterogeneity can also include the spatial variability of vessel density, perfusion, proton density and physiological tissue characteristics (Win et al., 2013; Asselin et al., 2012; Yoon et al., 2016).

In the recent years a lot of effort has been put into textural heterogeneity parameters as analyzed by PET-CT to assess tumor behavior and its responsiveness to therapy. One of the biggest reasons for this paradigm shift towards textural heterogeneity was that the conventional PET parameters which are usually considered as outcome predictors in clinical as well as research studies failed to provide sufficient information regarding various properties of tumor (O'Sullivan et al., 2003). These conventional parameters include maximum or mean standardized uptake value (SUV_{max} and SUV_{mean}) or the metabolically active tumor volume (MATV). Some of these properties, such as shape and uptake

heterogeneity, may reflect different tumor profiles associated with their aggressiveness, metastatic potential, or degree of response to a specific treatment, and consequently prognosis (Basu et al., 2011; Visvikis et al., 2012). However, quantification of these properties could provide information with higher clinical value than the usual metrics in selection of patients or identifying poor responders to treatment.

The use of textural analysis in the evaluation of PET images was first shown by El Naqa and colleagues in a seminal study in 9 patients with head and neck cancer and 14 patients with cervix cancer (El Naqa et al., 2009). Study comprised of investigating intensity-volume histogram metrics and shape and texture features extracted from PET images to predict patient's response to treatment. The preliminary results suggested that the proposed approaches could potentially provide better tools and discriminant power for utilizing functional imaging in clinical prognosis. Only two other studies investigating textural analysis in PET were published in the two following years. The first demonstrated the impact of parameters used in PET iterative image reconstruction algorithms on textural analysis metrics, of which many were shown to be sensitive to the resulting varying characteristics of the reconstructed images (Galavis et al., 2010). The second study investigated the predictive value of FDG uptake heterogeneity quantified using textural analysis, in 41 patients with locally advanced oesophageal cancer receiving concomitant chemoradiotherapy, and showed that textural analysis metrics have higher predictive value than SUV (Tixier et al., 2011).

In CT and MRI images several studies have shown that the textural analysis can be linked at the level of genomics through some pathophysiological processes constantly altering the innate tumor behavior. These studies (Segal et al., 2007; Gevaert et al., 2014; Wan et al., 2016) are very relevant for assessment of clinical data. A study established a correlation between perfusion CT-derived parameters (e.g. blood flow) and texture analysis metrics from FDG PET in stage HI/TV colorectal tumor’s (Tixier et al., 2014). Regarding the relationship between PET textural analysis features and data from underlying scales, preliminary results from a prospective study in 54 patients with head and neck cancer have

recently been presented, and demonstrate that some PET textural analysis metrics could be linked to altered signaling pathways related, for example, to cell proliferation and apoptosis (Tixier et al., 2015).

Studies like these can help us understand the added advantage of tumor textural analysis over the conventional PET parameters, which enhances the clinical value of the studies. However, major number of studies available are performed with FDG-PET. In our analysis to see the sensitivity and specificity of textural analysis in other radiotracers we used ^{18}F-FET PET and ^{68}Ga-PSMA PET. This was done in order see the predictive ability of this analysis with a varied number of radiotracers and also to study the tumoral variation and treatment response in different tumors. Depending on radiotracer and patient population our study was divided in three parts. We will individually discuss each of those.

Objective of the first part of study was to distinguish between true tumor progression and pseudoprogression in the patients of high grade glioma in FET-PET using textural heterogeneity parameters as compared to the conventional PET parameters. As described earlier the accurate and timely distinction between actual tumor progression and pseudoprogression (which is a sequel of chemoradiation) is very important, as it can effect significantly on further therapy planning and patient outcome.

The results of this study suggested that high grade glioma patients with suspected pseudoprogression could be classified into 3 distinct clusters, solely based on a set of textural FET-PET features. Most of the patients assigned to cluster 3 had pseudoprogression while all patients assigned to cluster 2 had true tumor progression. Thus, textural FET-PET feature analysis lent itself as a novel useful non-invasive tool, besides the frequently used TNRmax to distinguish pseudoprogression from true tumor progression in patients with high grade glioma.

When we compared the value of pseudoprogression prediction using a cluster-based classifier (cluster 3), that was based on textural PET features, against the most widely used

PET marker TNRmax (Galldiks et al., 2015; Kebir et al., 2016) only the cluster-based classifier was significantly associated with pseudoprogression detection. In the study (Galldiks et al., 2015) the objective was to assess the clinical value of O-(2-(18)F-fluoroethyl)-L-tyrosine^{18}F-FET PET in the differentiation of pseudoprogression and early tumour progression after radiochemotherapy of glioblastoma. A group of 22 glioblastoma patients with new contrast-enhancing lesions or lesions showing increased enhancement (>25 %) on standard MRI within the first 12 weeks after completion of radiochemotherapy with concomitant temozolomide (median 7 weeks) were additionally examined using amino acid PET with ^{18}F-FET. Maximum and mean tumour-to-brain ratios (TBRmax, TBRmean) were determined. Classification as pseudoprogression or actual tumor progression was based on the clinical course (no treatment change at least for 6 months), follow-up MR imaging and/or histopathological findings. Pseudoprogression was confirmed in 11 of the 22 patients. In patients with pseudoprogression, ^{18}F-FET uptake was significantly lower than in patients with actual progression (TBRmax 1.9 ± 0.4 vs. 2.8 ± 0.5, TBRmean 1.8 ± 0.2 vs. 2.3 ± 0.3; both $P < 0.001$) and presence of MGMT promoter methylation was significantly more frequent ($P = 0.05$). Receiver operating characteristic analysis showed that the optimal (18)F-FET TBRmax cut-off value for identifying pseudoprogression was 2.3 (sensitivity 100 %, specificity 91 %, accuracy 96 %, AUC 0.94 ± 0.06; $P < 0.001$). In comparison to that in our study the negative predictive value was higher with the cluster-based classifier, cluster 3.

Out of a set of 19 FET-PET features encompassing conventional (among others TLU, TNRmax, and TNRmean) as well as textural features, only 10 features separated all 3 clusters from one another. Of those 10, 7 features, namely Contrast, Volume, Entropy, TLU, Correlation, Size-zone var., and Coarseness were most differentially regulated among clusters and all of the latter 7 – except for TLU and Volume - are considered textural PET markers (30). These textural features reflect intratumoral uptake heterogeneity and may be used to quantify tumor heterogeneity (Tixier et al., 2011). The degree of intratumoral heterogeneity is suspected to be a prognostic factor (Almendro et al., 2013). Some textural markers such as Entropy and COV have been shown to be prognostically relevant in

systemic tumors (Almendro et al., 2013). Intriguingly, cluster 2, which included only patients with true progression, exhibited high values of heterogeneity markers (particularly Contrast and Entropy). By contrast, cluster 3, which included largely patients with confirmed pseudoprogression, was associated with low values of heterogeneity markers. On the other hand, TLU, the only non-textural marker of the 7 highly differentially regulated FET-PET-features, has been shown to be negatively correlated with prognosis and - compared to other conventional PET features - a stronger predictor of outcome in systemic tumors (Hyun et al, 2016; Choi et al., 2013). Interestingly, TLU was inversely associated with cluster 3, supporting that the cluster assignment based on our set of PET features might carry prognostic implications.

Similarly, in a recently published retrospective study (Pyka et al., 2016) of patients with high grade glioma, who received FET-PET prior to first-line treatment, 3 of the textural markers assessed here, namely complexity, contrast and coarseness, were shown to be possibly correlated with survival. All patients received static FET-PET scans prior to first-line therapy. TBR (max and mean), volumetric parameters and textural parameters based on gray-level neighborhood difference matrices were derived from static FET-PET images. All FET-PET textural parameters showed the ability to differentiate between World Health Organization (WHO) grade III and IV tumors ($p < 0.001$; AUC 0.775). Further improvement in discriminatory power was possible through a combination of texture and metabolic tumor volume, classifying 85 % of tumors correctly (AUC 0.830). Determination of uptake heterogeneity in pre-therapeutic FET-PET using textural features proved valuable for the (sub-)grading of high-grade glioma as well as prediction of tumor progression and patient survival, and showed improved performance compared to standard parameters such as TBR and tumor volume. In our very patient cohort, cluster 2 patients showed the lowest median PFS and OS compared to patients from the other clusters. Notably, canonical prognostic markers were similarly distributed among clusters and are not suited to explain this observation. However, survival times varied considerably among patients sharing the same cluster and the sample size was too small to draw strong conclusions from this pilot data. In addition, it should be mentioned that our cohort consisted of five patients who

underwent PET after relapse had occurred. With the other patients included in the first-line therapy, our cohort was heterogenous to some degree although those patients included after relapse were treated with again with alkylating (radio)chemotherapy. This cohort heterogeneity and the issue that treatment at recurrence might further account for varying PET data makes interpretation difficult. Nevertheless, because our findings might indicate a putatively prognostic value of clusters defined by textural FET-PET markers reflecting intratumoral uptake heterogeneity, a prospective study with a larger patient cohort validating our results is warranted.

In summary, this work provided a novel and interesting approach to FET-PET based identification of pseudoprogression from actual tumor progression. The textural heterogeneity can be easily incorporated into routine PET investigations. The ability of the study to provide us with this important discrimination can give a lot of clinical benefit. Patients with diagnosis of actual tumoral progression can undergo further therapy resulting in decreased morbidity and mortality, while patients with a true diagnosis of pseudoprogression can then avoid undergoing any unnecessary treatment. However, as mentioned above, by virtue of the small sample size interpretation of our results is limited and calls for validation in larger and systemic analyses. Nevertheless, this approach is novel, the results are promising, and encourage analyzing the diagnostic value of textural markers in a larger cohort of patients.

In the second and third parts of our study, we analyzed the predictive capability of textural heterogeneity parameters in patients undergoing ^{177}Lu-PSMA therapy for determination of patient selection criteria, treatment outcome and survival analysis.
PSMA bound ligands have started gaining acceptance for diagnosis and treatment of prostate cancer (Rahbar et al., 2017; Kulkarni et al., 2016; Baum et al., 2016). The retrospective German multicenter analysis (Rahbar et al., 2017) showed that ^{177}Lu-PSMA-617 radioligand therapy demonstrated favorable safety and high efficacy exceeding those of other third-line systemic therapies in metastatic castration resistant prostate cancer patients. PSA decline occurred in 65% of patients after 1 cycle of radioligand therapy with

^{177}Lu-PSMA-617 and in 72% after the second cycle. There are still almost 30% of the patients who did not show or showed less than 50% decline in serum PSA level. It is very important to identify those patients and so that therapy modifications might be performed which can then help in increasing the efficacy of treatment. Our study aimed at utilization of heterogeneity parameters in an effort to improve the selection criterion of patients and acted as a means to predict improved outcome. To achieve this effect at the earliest possible time, prior to therapy planning analysis was performed on the data collected from baseline scan. Our study showed a potential for response prediction through baseline PSMA-PET-CT scan using textural features. It also suggested that more heterogeneous the tumor was in PSMA expression more responsive it was to PSMA therapy, thus contributing efficiently towards patient selection, treatment planning and improvement in overall diagnostic accuracy. The ROC analysis showed that two textural heterogeneity parameters entropy and homogeneity were statistically significant ($p < 0.05$) for predictive ability as obtained from the baseline ^{68}Ga-PSMA scan prior to ^{177}Lu-PSMA therapy. Spearman correlation showed that entropy showed a negative correlation ($r_s = -0.327$ and $p = 0.006$) and homogeneity showed a positive correlation ($r_s = 0.315$ and $p = 0.008$) with change in pre and post therapy PSA levels.

Predictive ability of various parameters from the baseline scan has also been investigated. In a study (Ferdinandus et al., 2017) the effect of different pretherapeutic parameters on the therapeutic response measured by prostate-specific antigen (PSA) 2 months after radioligandtherapy. In the univariate analysis, younger age, higher levels of γ-glutamyl transferase, lower pretherapeutic hemoglobin, a higher Gleason score, a higher number of platelets, higher C-reactive protein, regular need for pain medication, and higher lactate dehydrogenase had a negative impact on the therapeutic response; however, the multivariate analysis revealed that the most significant independent factors were the number of platelets and regular need for pain medication. The response was independent of the amount of PSMA uptake as well as previous therapies and other measured factors. A PSA decline of more than 50% was observed significantly more in patients without a regular need for analgesics. Numerous studies have also reported the use of textural

heterogeneity parameters for the assessment of patient outcome. PET due to its ability for physiological imaging and hence having the ability to predict changes at molecular level and also having the added advantage of whole body imaging is an ideal choice for analyzing textural heterogeneity parameters.

A study (Eary et al., 2008) proposed that heterogeneity in ^{18}F-FDG spatial distribution can be used to predict tumor biologic aggressiveness. This study presented data to support the hypothesis that a new heterogeneity-analysis algorithm applied to ^{18}F-FDG PET images of tumors in patients was predictive of patient outcome. ^{18}F-FDG PET images from 238 patients with sarcoma were analyzed using a new algorithm for heterogeneity analysis in tumor ^{18}F-FDG spatial distribution. Statistical analyses show that heterogeneity analysis is a strong independent predictor of patient outcome**.** The new ^{18}F-FDG PET tumor image heterogeneity analysis method was validated for the ability to predict patient outcome in a clinical population of patients with sarcoma. It was proposed that this method could be extended to other PET image datasets in which heterogeneity in tissue uptake of a radiotracer may predict patient outcome.

In another study (Cheng et al., 2013) the researchers investigated whether the textural features of pretreatment ^{18}F-FDG PET-CT images could provide any additional prognostic information and clinical staging in patients with advanced T-stage oropharyngeal squamous cell carcinoma. Retrospective analysis of the pretreatment ^{18}F-FDG PET-CT images of 70 patients was performed. The textural features of pretreatment ^{18}F-FDG PET-CT images were extracted from histogram analysis (SUV variance and SUV entropy), normalized gray-level cooccurrence matrix (uniformity, entropy, dissimilarity, contrast, homogeneity, inverse different moment, and correlation), and neighborhood gray-tone difference matrix (coarseness, contrast, busyness, complexity, and strength). Receiver-operating-characteristic curves were used to identify the optimal cutoff values for the textural features. Multivariate Cox regression analysis showed that age, tumor TLG, and uniformity were independently associated with progression-free survival (PFS) and disease-specific survival (DSS). TLG, uniformity, and HPV positivity were significantly associated

with overall survival (OS). A prognostic scoring system based on TLG and uniformity was derived. Uniformity extracted from the normalized gray-level co-occurrence matrix represented an independent prognostic predictor in patients with advanced T-stage oropharyngeal squamous cell carcinoma. A scoring system was developed and that might serve as a risk-stratification strategy for guiding therapy. In our study we also analyzed pretreatment ^{68}Ga-PSMA scans of 70 patients. Two textural heterogeneity parameters entropy and homogeneity showed ability to predict outcome. However, the conventional PET parameters SUV mean and max did not show such ability. Tumor volume also had no effect on textural heterogeneity.

Similarly in another study (Tixier et al., 2011) the aim was to propose and evaluate new parameters obtained by textural analysis of baseline PET scans for the prediction of therapy response in esophageal cancer. Forty-one patients with newly diagnosed esophageal cancer treated with combined radiochemotherapy were included in this study. All patients underwent pretreatment whole-body ^{18}F-FDG PET. Different image-derived indices obtained from the pretreatment PET tumor images were considered. These included usual indices such as maximum SUV, peak SUV, and mean SUV and a total of 38 features (such as entropy, size, and magnitude of local and global heterogeneous and homogeneous tumor regions) extracted from the 5 different textures considered. The capacity of each parameter to classify patients with respect to response to therapy was assessed using the Kruskal-Wallis test ($P < 0.05$). Specificity and sensitivity (including 95% confidence intervals) for each of the studied parameters were derived using receiver-operating-characteristic curves. Relationships between pairs of voxels, characterizing local tumor metabolic non uniformities, were able to significantly differentiate all 3 patient groups ($P < 0.0006$). Regional measures of tumor characteristics, such as size of non-uniform metabolic regions and corresponding intensity non-uniformities within these regions, were also significant factors for prediction of response to therapy ($P = 0.0002$). Receiver-operating-characteristic curve analysis showed that tumor textural analysis can provide non-responder, partial-responder, and complete-responder patient identification with higher sensitivity (76%-92%) than any SUV measurement. Textural features of tumor metabolic

distribution extracted from baseline ^{18}F-FDG PET images allow for the best stratification of esophageal carcinoma patients in the context of therapy-response prediction. In our study the combined sensitivity of entropy and homogeneity for predicting outcome was 57.8% and the combined specificity was 87.7%.

It is interesting to note that in our results entropy showed a directly proportional correlation with change in pre and post therapy PSA levels while homogeneity showed an inverse relationship. In other words it can be inferred that more heterogeneous the tumor was, the better it responded to the PSMA therapy. As higher entropy is a measure of greater heterogeneity of the tumor. The patients which were labeled as responders owing to decrease in post PSMA therapy PSA levels showed a higher entropy in baseline scan. Similarly, the responders showed lower homogeneity in the baseline scan. Although we did define the response to therapy by PSA levels and did not correlate the textural features with patient outcomes, we have shown in previous studies, that a reduction of PSA after therapy with Lu-177 PSMA is a prognostic factor for overall survival (Ahmadzadehfar et al., 2016; Ahmadzadehfar et al., 2017).

In the study by Pyka T et.al. (Pyka et al., 2015), they evaluated the predictive value of textural heterogeneity parameters in FET-PET for recurrence and prognosis in non-small cell lung carcinoma (NSCLC) patients receiving primary stereotactic radiation therapy (SBRT). 45 patients with early stage NSCLC (T1 or T2 tumor, no lymph node or distant metastases) were included in this retrospective study and followed over a median of 21.4 months (range 3.1–71.1). Pre-treatment FDG-PET/CT scans were obtained from all patients. SUV and volume-based analysis as well as extraction of textural features based on neighborhood gray-tone difference matrices (NGTDM) and gray-level co-occurence matrices (GLCM) were performed using InterView Fusion™ (Mediso Inc., Budapest, Hungary). ROC revealed a significant correlation of several textural parameters with local recurrence with an AUC value for entropy of 0.872. While there was also a significant correlation of local recurrence with tumor size in the overall cohort, only texture was predictive when examining T1 (tumor diameter < = 3 cm) and T2 (>3 cm) subgroups. In

univariate survival analysis, both heterogeneity and tumor size were predictive for disease-specific survival, but only texture determined by entropy was determined as an independent factor in multivariate analysis (hazard ratio 7.48, p = .016). Overall survival was not significantly correlated to any examined parameter, most likely due to the high comorbidity in our cohort. This study showed that entropy has predictive potential for local recurrence with an AUC of 0.872. The study also showed that higher value of entropy was linked to poor outcome. In our study entropy was also a predictor for outcome with an AUC of 0.695 however, higher entropy showed better outcome for PSMA therapy. Similarly, another study (Soussan et al., 2014) discussed whether tumor heterogeneity measured using texture analysis in FDG-PET images is correlated with pathological prognostic factors in invasive breast cancer. Fifty-four patients with locally advanced breast cancer who had an initial FDG-PET were retrospectively included. In addition to SUVmax, three robust textural indices extracted from 3D matrices: High-Gray-level Run Emphasis (HGRE), Entropy and Homogeneity were studied. Univariate and multivariate logistic regression was used to identify PET parameters associated with poor prognosis pathological factors: hormone receptor negativity, presence of HER-2 and triple negative phenotype. Receiver operating characteristic (ROC) curves and the (AUC) analysis, and reclassification measures, were performed in order to evaluate the performance of combining texture analysis and SUVmax for characterizing breast tumors. Results showed that triple negative breast cancer (TNBC) exhibited higher SUVmax, lower Homogeneity non-TNBC. Tumor heterogeneity measured on FDG-PET was higher in invasive breast cancer with poor prognosis pathological factors. Texture analysis might be used, in addition to SUVmax, as a new tool to assess invasive breast cancer aggressiveness. In this study lower homogeneity was associated with poor outcome of breast cancer patients. However in our study lower homogeneity (AUC 0.683) was associated with better outcome.

An interesting question which arises here is whether a more heterogeneous tumor can respond better to the treatment? In many previous studies involving textural heterogeneity it was proven otherwise. Increased textural heterogeneity has already been linked with poor outcome. On the contrary, our study points in the opposite direction. One of

the reasons for this behavior could be that this phenomenon can possibly be highly tumor and therapy specific. PSMA shows significant over expression in metastatic, poorly differentiated and therapy refractory carcinomas. Treatment refractory tumors can have the presence of multiple clones resulting in formation of complex systems and contributing towards tumor heterogeneity (Ahmadzadehfar et al., 2016). Patients included in our study group had already metastatic disease which was treatment refractory. Therefore, we can assume that there was a significant PSMA overexpression in tumors of patients included in our study. More heterogeneous a tumor is, more PSMA expression it shows thereby increasing the uptake of PSMA bound ligands and thus responding better to therapy. In a very interesting study by Jeffrey West and Paul Newton (West and Newton, 2017) about Optimizing chemo-scheduling based on tumor growth rates discussed ways to optimize chemotherapeutic scheduling using a Moran process evolutionary game-theory model of tumor growth that incorporates more general dynamical and evolutionary features of tumor cell kinetics.

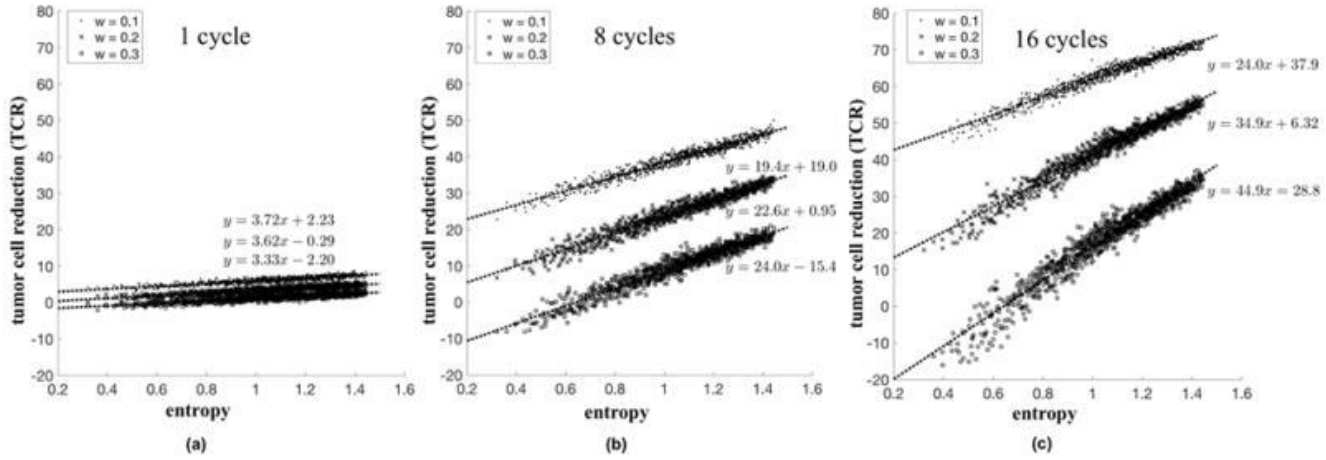

ill. 13: The relationship between tumor cell reduction (TCR) and entropy (H) is shown for a single cycle of chemotherapy (a), 8 cycles (b), and 16 cycles (c). The low slope value in (a) indicates negligible advantage of high entropy strategies after only a single cycle. After many cycles, the advantage of high entropy strategies is apparent (b,c).

Using this model, and employing the quantitative notion of Shannon entropy they found out that which assigns high values to low-dose metronomic (LDM) therapies, and low values to maximum tolerated dose (MTD) therapies, we show that low-dose metronomic strategies can outperform maximum tolerated dose strategies, particularly for faster growing tumors. It proves the fact that over multiple cycles, higher entropy strategies have a bigger impact on faster growing tumors than on slower growing tumors.

Our study showed as well that more heterogeneous a tumor is in PSMA expression better it responses to PSMA therapy. Higher entropy and lower homogeneity proved to be good predictors for favorable outcome. This could be especially important for patients with hormone treatment refractory prostate cancers which have already undergone multiple therapies prior to PSMA therapy and the resulting poor differentiation results in increased heterogeneity in cancer cells. PSMA with its specific property of over expression in hormone refractory, poorly differentiated and metastatic cancers can hence show better therapy response in such cases. All the patients in our study which were candidates for PSMA therapy were labeled as refractory to hormone treatment and several had undergone some other treatment options before as well. As, PSMA serves as a target of targeted therapy with ^{177}Lu-PSMA, its over expression might result in better uptake of radiopharmaceutical. So, in pre-therapy analysis the patients with lesions having higher entropy and intensity variation and less homogeneity proved to be better targets for therapy and responded more to treatment.

Hence, firstly this study showed the possibility of extracting vital data via the analysis of baseline scan only which can directly predict the outcome of patient. This finding can be of excessive importance in selecting the patients which can possibly respond better by altering the treatment regimen. Secondly, this study differentiates the textural parameters which can be used for gaining outcome data and also points out their correlation with the outcome.

In the third part of our research, we analyzed the capability of textural inhomogeneity markers on PET to predict therapy response and outcome in patients with hormone refractory prostate carcinoma. The markers analyzed were determined before, during, and after completion of three ^{177}Lu-PSMA therapies. Regarding the predictive capability, three parameters entropy, homogeneity and intensity variation showed statistical significance in all stages of study. For personalized therapy it is very important if outcome can be predicted in the start of therapy. The earlier the outcome is predicted the more beneficial it is for the patient. In the pre-therapy analysis entropy had the highest AUC (0.72) and a sensitivity of 95%. In the mid-therapy analysis again entropy showed the highest AUC (0.67). However, it was less than that of pre-therapy analysis. The highest specificity was showed by homogeneity in both pre and mid-therapy analyses. In the post-therapy analysis homogeneity showed the highest AUC (0.755). The highest specificity was again showed by homogeneity while entropy showed maximum sensitivity. We also showed that there was no correlation between lesion volume and any of the positive parameters throughout the course of study. Numerous studies have investigated the predictive value of textural heterogeneity parameters for assessment of therapy response.

In a study Lapa C. et. Al.,(Lapa et al., 2015) investigated the potential of somatostatin receptor subtype II (SSTR)-PET to assess intraindividual tumor heterogeneity and thereby treatment response prior to peptide receptor radionuclide therapy (PRRT).12 patients with progressive radioiodine-refractory differentiated or medullary thyroid cancer were enrolled. SSTR-PET was performed at baseline. Conventional PET parameters and heterogeneity parameters were analyzed regarding their potential to predict progression-free (PFS, mean, 221 days) and overall survival (OS, mean, 450 days).In patient-based analysis, all conventional parameters failed to predict PFS. Several textural parameters showed a significant capability to assess PFS. Thereby, "Grey level non uniformity" had the highest area under the curve (AUC, 0.93) in Receiver operating characteristics analysis followed by "Contrast" (AUC, 0.89). In lesion-based analysis, only "Entropy" revealed potential to evaluate disease progression. OS could not be assessed by any parameter investigated. It was concluded that tumor heterogeneity seems to be a predictor of

response to PRRT in patients with iodine-refractory differentiated/advanced medullary thyroid cancer and outperforms conventional PET parameters like standardized uptake value. In another study by Bundschuh et. Al., (Bundschuh et al, 2014) investigated textural parameters for their predictive and prognostic capability in patients with rectal cancer using histopathology as the gold standard. In addition, a comparison to clinical outcome was performed. Twenty-seven patients with rectal cancer underwent ^{18}F-FDG PET-CT before, 2 weeks after the start, and 4 weeks after the completion of neoadjuvant chemoradiotherapy. In all PET-CT scans, conventional parameters (tumor volume, diameter, maximum and mean standardized uptake values, and total lesion glycolysis [TLG]) and textural parameters (coefficient of variation [COV], skewness, and kurtosis) were determined to assess tumor heterogeneity. The COV showed a statistically significant capability to assess histopathologic response early in therapy (sensitivity, 68%; specificity, 88%) and after therapy (79% and 88%, respectively). Thereby, the COV had a higher area under the curve in receiver-operating-characteristic analysis than did any analyzed conventional parameter for early and late response assessment. The COV showed a statistically significant capability to evaluate disease progression and to predict survival, although the latter was not statistically significant. In our study, the predictive value of parameters and the defining parameters were different from that in the studies mentioned above. The differences can be because of different tumor type and different therapeutic agents. However, the findings of our study correspond to the results of all the above mentioned studies in the aspect that in that tumor heterogeneity was a better parameter for prediction of therapy response than the conventional parameters SUVmax, SUVmean, and lesion size.

In the study entropy was the parameter with highest p-value and thus potential for best predictive capability in pre-therapy analysis for identifying high risk patients and those for whom therapy will be effective. Similarly, for post-therapy analysis entropy had highest p-value for identifying patients with high risk for disease progression and death, followed by intensity variation and homogeneity.

The changes in textural heterogeneity showed a very interesting pattern throughout the course of study. For the pre-therapy analysis the lesions which showed greater entropy and intensity variation and lesser homogeneity showed better predictive potential. Meaning that the more heterogeneous a tumor was better response it was showing to therapy, as increased entropy and intensity variation are directly proportional to the heterogeneity of a tumor. This particular point has been discussed in detail in the previous section of discussion. However, in the analysis of post therapy scan (after three therapies) it was observed that the patients who had decreased tumor textural heterogeneity showed a survival potential than those who showed persistently high textural heterogeneity. So, after three therapies patients with lower entropy and intensity variation and higher homogeneity showed better outcome and potential for survival than those showing persistently higher entropy and intensity variation and lower homogeneity. It could show that during the course of treatment PSMA therapy effectively brought some changes to the texture of tumor which resulted in increased homogeneity to tumor texture. There is published data analyzing the effects of chemo or radiation therapy on tumors at molecular and genetic level. As also described in introduction the origin of textural heterogeneity in tumors can be traced to molecular and genetic level, hence they can be good depicters of changes brought along by therapy at these levels.

A study (Zeng et al., 2011) showed interactions between various genes and radiotherapy and chemotherapy. 211 patients with pancreatic cancer were recruited in a population-based study. Sixty-four candidate genes associated with cancer survival or treatment response were selected from existing publications. The main effect of genetic variation and gene-specific treatment interactions on overall survival were examined by proportional hazards regression models. In a recent study (Bravatà et al.,2018) evidence was given of the substantial alterations in gene expression levels and pathways after ionizing radiation treatment in both immortalized and primary cell cultures. Overall, the ionizing radiation-induced gene expression profiles and pathways appear to be cell-line dependent. The data suggest that some specific gene and pathway signatures seem to be linked to hormone receptor status. These findings show that not only radiotherapy brought

changes into tumor behavior at molecular level but also that these changes were very specific for tumor type. Hence, tumors with increased PSMA expression can behave in an entirely different way than other tumoral cell lines. The lesions which were more heterogeneous before the start of therapy in our study responded better to treatment owing to specific characteristics of both tumor and tracer but during the course of treatment the therapy gradually changed the characteristics of tumor and hence the survival potential. These findings are in accordance with the results obtained through numerous studies mentioned before which conclude that increased textural heterogeneity is a poor predictor to treatment response and overall survival.

These findings also suggest that every tumor has a very unique and individual behavior and textural parameters can not only help in predicting that behavior but also can determine the patient outcome and disease progression. Therefore, these parameters can be an important part of personalized therapy. These are very important findings to understand the subsequent effects of a therapy on tumoral behavior. Persistent heterogeneity after multiple therapies and thus poor outcome can lead to the inference that there might be some resistant clones not responding to therapy and thus can be labeled as non-responders.

Our study provided some good data on the role of tumor textural heterogeneity in predicting treatment outcome, overall survival, selection criteria for patients and to differentiate between actual and pseudo progression (in the case of high grade gliomas). Textural parameters in these ways can provide us with useful clinical information. It can help in identifying non-responders to treatment and can also help in distinguishing the patients who can respond better to a specific therapy. Textural heterogeneity parameters can influence the decision making in therapy planning by providing better identification of responders. It can serve as a basis for personalized therapy. Personalized therapy is now gaining a lot of importance for increasing the efficacy of treatments and modifying therapy options in order to provide patients with more effective treatment options. Analysis of

textural heterogeneity parameters can help in achieving these goals and can directly affect the outcome of patient which can result in significant decrease in disease burden.

This study had some limitations. First, the reproducibility of tumor heterogeneity as assessed by PSMA PET-CT has not been much explored yet. For the assessment of this robustness repeated analysis of PSMA PET-CT studies will have to be performed in a short interval of time. For FDG-PET-CT, such a study has been performed by Tixier et al. and demonstrated reproducibility of textural parameters comparable to the range of conventional SUV (Tixier et al., 2011). They found that several textural parameters showed reproducibility comparable to the range of conventional SUV. Therefore, these parameters can be applied for therapy response assessment at least with the same confidence as SUV. However, this result should be validated by further studies. The analysis of heterogeneity can also be limited by the size of the lesion. If the lesion becomes too small, the analysis of differences in radiotracer uptake within the lesion does not make sense. Investigating small structures, e.g. lymph node metastases, may challenge the value of textural parameters. In our study, the smallest lesion was 8.7 cm3, which is still about 62 voxels. A second point that needs further investigation is the influence of reconstruction parameters on tissue heterogeneity. PET reconstruction algorithms require smoothing of the raw image data which could influence assessment of tumor textural heterogeneity. PET images assessed in this study were reconstructed using the standard protocols for clinical routine at our institution. For comparison of changes in tumor heterogeneity, all images were acquired and reconstructed with the same set of parameters. In a study (Yan et al., 2015), it has been shown that the impact of reconstruction settings on texture parameters is unclear, especially relating to time-of-flight (TOF) and point-spread function (PSF) modeling. Their effects on 55 texture features (TF) and 6 features based on first-order statistics (FOS) were investigated. Standardized uptake value (SUV) measures were also evaluated as peak, maximum and mean SUV. The coefficient of variation (COV) of each feature across different reconstructions was calculated. Results showed that Peak SUV, mean SUV, 18 TFs and 1 FOS were the most robust (COV≤5%). The features which exhibited large variation such as skewness in FOS, cluster shade and zone percentage

should be used with caution. The entropy in FOS, difference entropy, inverse difference normalized, inverse difference moment normalized, low grey-level run emphasis, high grey-level run emphasis and low grey-level zone emphasis are the most robust features. Similarly, in another study (Morita et al., 2016) **t**he purpose was to examine the effects of different reconstruction algorithms on the degree of heterogeneity of FDG uptake as assessed by texture analysis. The heterogeneity of the ^{18}F distribution was evaluated according to fourteen texture features on a SUV histogram, a co-occurrence matrix (NGLCM), and a neighborhood gray-tone difference matrix (NGTDM). This was obtained using different algorithms on a phantom. In the comparison between ordered-subsets expectation maximization (OSEM) and time-of-flight (TOF), thirteen features, including two SUV histogram features, seven NGLCM features and four NGTDM features showed similar patterns. On the other hand, in the comparison between OSEM and point-spread function PSF, six features, including one SUV histogram feature, one NGLCM feature and four NGTDM features showed similar patterns. In the comparison between PSF and PSF+TOF, thirteen features, including two SUV histogram features, seven NGLCM features and four NGTDM features showed similar patterns. TOF correction did not influence the evaluation of the heterogeneity on PET images, while PSF correction affected the evaluation of heterogeneity. In our studies we have used the textural parameters which are robust as analyzed by several algorithms.

Furthermore, as another drawback of this study, metabolically active tumor volumes were delineated manually instead of using segmentation algorithms with fixed thresholds and might therefore be prone to interindividual differences. However, the appropriate segmentation method is still widely discussed; semiautomatic methods often fail depending on the tumor localization (Zaidi et al., 2012; Bundschuh et al., 2012). Therefore, we considered manual delineation to be optimal for our study especially as we included metastases varying in location as well as signal-to-background ratio. Additionally, Hatt and colleagues (Hatt et al., 2013) could demonstrate that the predictive value of textural parameters is not affected by partial volume effect and is relatively independent of the method used to delineate the tumor volumes to be analyzed.

5. Abstract

Introduction: PET-CT is emerging to be the most efficient tool for tumor diagnosis and therapy monitoring. Some newer techniques like analysis of tumoral textural heterogeneity via PET are proving to be more effective than conventional PET parameters for diagnosis, patient selection and treatment planning. We carried out this study to analyze the role of textural heterogeneity parameters in improving the specificity of PET scans. The study was divided in three parts. In the first part, we explored the role of textural features in FET-PET for early detection of pseudoprogression in high grade gliomas as timely detection of pseudoprogression is crucial for the management of patients with HGG. In the second part, the objective was to assess the predictive ability of tumor textural heterogeneity parameters from baseline ^{68}Ga-PSMA PET for patient selection prior to ^{177}Lu-PSMA therapy. This could prove essential for response prediction and risk stratification of patients before the start of therapy resulting in better treatment outcome. Purpose of the third part of study was to investigate the role of tumor heterogeneity in pre and post therapy ^{68}Ga-PSMA scans for early response prediction and estimation of over-all survival in patients with ^{177}Lu-PSMA therapy. **Materials and methods:** For distinction between PsP and actual tumor progress fourteen patients with HGG and suspected of PsP underwent FET-PET. A set of 19 conventional and textural FET-PET features were evaluated and subjected to unsupervised consensus clustering and cluster stability assessment. The nearest shrunken centroids method was applied to determine the most relevant features underlying each cluster. The final diagnosis of true progression vs. PsP was based on follow-up MRI using RANO criteria. In the second part of study, retrospective analysis of 70 patients with mCRPC was performed. Five PET based textural heterogeneity parameters (COV, entropy, homogeneity, contrast, size variation) were determined in baseline ^{68}Ga-PSMA scan. Results obtained were then compared with clinical parameters including pre and post therapy PSA, alkaline phosphate, bone specific alkaline phosphate levels and ECOG criteria. Spearman correlation was used to determine statistical dependence among variables. ROC analysis was performed to estimate the optimal cutoff value and AUC. In the third part of study, retrospective analysis of 50 patients undergoing ^{177}Lu-PSMA therapy

was performed. Pre-therapy, mid-therapy and post-therapy scans were used for analysis. In addition to conventional parameters, 5 PET based textural heterogeneity parameters were determined. ROC and Kaplan-Meier analyses were used for response assessment, time to progression and survival. **Results:** For differentiation of PsP, three robust clusters were identified. None of the patients with PsP fell into cluster 2, which was associated with high values for textural FET-PET markers. Three out of 4 patients with PsP were assigned to cluster 3 that was largely associated with low values of textural FET PET features. In comparison, tumor-to-normal ratio (TNRmax) at optimal cut-off 2.1 was less predictive of PsP (negative predictive value 57% for detecting true progression, p=0.07 vs. 75% with cluster 3, p=0.04). Furthermore, patients in cluster 2 were associated with a comparably lower progression-free survival. In the second part of study, in bone lesions entropy showed a negative correlation (r_s = -0.327, p = 0.006, AUC = 0.695) and homogeneity showed a positive correlation (r_s = 0.315, p = 0.008, AUC = 0.683) with change in pre and post therapy PSA levels. Other parameters did not show statistically significant correlations. It suggested that the more heterogeneous the tumor was in PSMA expression the more responsive it was to PSMA therapy. For the third part of study, in bone lesions entropy, homogeneity and intensity variation (AUC 0.725, 0.679, 0.716 respectively) showed statistically significant ability to predict response prediction. Entropy showed highest statistically significant capability to evaluate disease progression and to predict survival. In pre-therapy analysis the lesions with higher textural heterogeneity showed better response to treatment, however after 3 therapies patients having lesions with persistently high textural heterogeneity showed poor prognosis and survival. **Conclusions:** Textural heterogeneity parameters helped in distinguishing PsP from actual progress thus plying an essential role in therapy planning and patient outcome. For ^{177}Lu-PSMA therapy our study showed a potential for response prediction through one baseline Ga-68-PSMA scan only. It also predicted which patients could respond better to the therapy thus forming selection criteria for patients that can help in better treatment planning for individual patients. In analysis of pre and post therapy data for the third part of study, tumor heterogeneity analysis proved to be superior to the investigated conventional parameters, as an important predictive factor in determining the therapy response and overall survival of patients.

6. List of figures

7. List of tables

9. References

Aerts HJ, Velazquez ER, Leijenaar RT, Parmar C, Grossmann P, Carvalho S, Bussink J, Monshouwer R, Haibe-Kains B, Rietveld D, Hoebers F, Rietbergen MM, Leemans CR, Dekker A, Quackenbush J, Gillies RJ, Lambin P. Decoding tumour phenotype by noninvasive imaging using a quantitative radiomics approach. Nat Commun 2014; 5:4006

Afshar-Oromieh A, Malcher A, Eder M, et al. PET imaging with a [68Ga]gallium labelled PSMA ligand for the diagnosis of prostate cancer: biodistribution in humans and first evaluation of tumour lesions. Eur J Nucl Med Mol Imaging. 2013; 40:486–495

Ahmadzadehfar H, Eppard E, Kürpig S, Fimmers R, Yordanova A, Schlenkhoff CD, et al. Therapeutic response and side effects of repeated radioligand therapy with 177 Lu-PSMA-DKFZ-617 of castrate-resistant metastatic prostate cancer. Oncotarget. 2016; 7(11):12477-12488

Ahmadzadehfar H, Rahbar K, Kurpig S, et al. Early side effects and first results of radioligand therapy with 177Lu-DKFZ-617 PSMA of castrate-resistant metastatic prostate cancer: a two-centre study. EJNMMI Res 2015; 5:114

Ahmadzadehfar H, Wegen S, Yordanova A, Fimmers R, Kürpig S, Eppard E WX, Schlenkhoff C, Hauser S EM. Overall survival and response pattern of castration-resistant metastatic prostate cancer to multiple cycles of radioligand therapy using [(177)Lu]Lu-PSMA-617. Eur J Nucl Med Mol Imaging. 2017; 44(9):1448-1454

Al-Kadi OS. Assessment of texture measures susceptibility to noise in conventional and contrast enhanced computed tomography lung tumour images. Comput Med Imaging Graph 2010; 34(6):494–503

Al-Kadi OS, Watson D. Texture analysis of aggressive and nonaggressive lung tumor CE CT images. IEEE Trans Biomed Eng 2008; 55(7):1822–1830

Almendro V, Marusyk A, Polyak K. Cellular heterogeneity and molecular evolution in cancer. Annu Rev Pathol 2013; 8:277-302

Alobaidli S, McQuaid S, South C, Prakash V, Evans P, Nisbet A. The role of texture analysis in imaging as an outcome predictor and potential tool in radiotherapy treatment planning. Br J Radiol 2014t; 87(1042):20140369

Amadasun M, King R. Textural features corresponding to textural properties. IEEE Transactions on Systems, Man and Cybernetics. 1989; 19:1264–1274

Asselin MC, O'Connor JP, Boellaard R, Thacker NA, Jackson A. Quantifying heterogeneity in human tumours using MRI and PET. Eur J Cancer. 2012; 48:447–455

Basu S, Kwee TC, Gatenby R, Saboury B, Torigian DA, Alavi A. Evolving role of molecular imaging with PET in detecting and characterizing heterogeneity of cancer tissue at the primary and metastatic sites, a plausible explanation for failed attempts to cure malignant disorders. Eur J Nucl Med Mol Imaging. 2011; 38:987–991

Baum RP, Kulkarni HR, Schuchardt C, Singh A, Wirtz M, Wiessalla S, et al. ^{177}Lu-Labeled Prostate-Specific Membrane Antigen Radioligand Therapy of Metastatic Castration-Resistant Prostate Cancer: Safety and Efficacy. J Nucl Med 2016; 57(7):1006–1013

Benesová M, Schafer M, Bauder-Wust U, et al. Preclinical evaluation of a tailor-made DOTA-conjugated PSMA inhibitor with optimized linker moiety for imaging and endoradiotherapy of prostate cancer. J Nucl Med 2015; 56: 914–920

Bostwick DG, Pacelli A, Blute M, et al. Prostate specific membrane antigen expression in prostatic intraepithelial neoplasia and adenocarcinoma: a study of 184 cases. Cancer. 1998; 82:2256–2261

Brandsma D, Stalpers L, Taal W, Sminia P, van den Bent MJ. Clinical features, mechanisms, and management of pseudoprogression in malignant gliomas. Lancet Oncol 2008; 9:453–461

Bravatà V, Cava C, Minafra L, Cammarata FP, Russo G, Gilardi MC, Castiglioni I, Forte GI. Radiation-Induced Gene Expression Changes in High and Low Grade Breast Cancer Cell Types. Int J Mol Sci 2018; 19(4). pii: E1084

Brown RA, Frayne R. A comparison of texture quantification techniques based on the Fourier and S transforms. Med Phys 2008; 35(11):4998–5008

Bundschuh RA, Dinges J, Neumann L, Seyfried M, Zsótér N, Papp L, et al. Textural Parameters of Tumor Heterogeneity in 18F-FDG PET/CT for Therapy Response Assessment and Prognosis in Patients with Locally Advanced Rectal Cancer. J Nucl Med 2014; 55(6):891–897

Bundschuh RA, Andratschke N, Dinges J, Duma MN, Astner ST, Brugel M, et al. Respiratory gated [18F]FDG PET/CT for target volume delineation in stereotactic radiation treatment of liver metastases. Strahlenther Onkol 2012; 188:592–598

Castellano G, Bonilha L, Li LM, Cendes F. Texture analysis of medical images. Clin Radiol 2004; 59(12):1061–1069

Chang SS, Reuter VE, Heston WD, Gaudin PB. Comparison of anti-prostate-specific membrane antigen antibodies and other immunomarkers in metastatic prostate carcinoma. Urology. 2001; 57:1179–1183

Chaskis C, Neyns B, Michotte A, De Ridder M, Everaert H. Pseudoprogression after radiotherapy with concurrent temozolomide for high-grade glioma: clinical observations and working recommendations. Surg Neurol 2009; 72:423–428

Cheng NM, Dean Fang YH, Tung-Chieh Chang J, Huang CG, Tsan DL, Ng SH, et al. Textural Features of Pretreatment ^{18}F-FDG PET/CT Images: Prognostic Significance in Patients with Advanced T-Stage Oropharyngeal Squamous Cell Carcinoma. J Nucl Med 2013; 54(10):1703–1709

Choi ES, Ha SG, Kim HS, Ha JH, Paeng JC, Han I. Total lesion glycolysis by 18F-FDG PET/CT is a reliable predictor of prognosis in soft-tissue sarcoma. Eur J Nucl Med Mol Imaging. 2013; 40(12):1836-1842

Craciunescu OI, Das SK, Clegg ST. Dynamic contrast-enhanced MRI and fractal characteristics of percolation clusters in two-dimensional tumor blood perfusion. J Biomech Eng 1999; 121(5):480–486

Crocetti Emanuele. Epidemiology of prostate cancer in Europe. Center for parliamentary studies. 2015

Davnall F, Yip CS, Ljungqvist G, Selmi M, Ng F, Sanghera B, Ganeshan B, Miles KA, Cook GJ, Goh V. Assessment of tumor heterogeneity: an emerging imaging tool for clinical practice? Insights Imaging. 2012; 3(6): 573-589

Dettori L, Semler L. A comparison of wavelet, ridgelet, and curvelet-based texture classification algorithms in computed tomography. Comput Biol Med 2007; 37(4):486–498

Dick JE. Stem cell concepts renew cancer research. Blood. 2008; 112:4793–4807

Divrik RT, Türkeri L, Şahin AF, Akdoğan B, Ateş F, Çal Ç BS. Prediction of response to androgen deprivation therapy and castration resistance in primary metastatic prostate cancer. Urol Int 2012;88(1)

Dong X, Sun X, Sun L, Maxim PG, Xing L, Huang Y, Li W, Wan H, Zhao X, Xing L YJ. Early Change in Metabolic Tumor Heterogeneity during Chemoradiotherapy and Its Prognostic Value for Patients with Locally Advanced Non-Small Cell Lung Cancer. PLoS One. 2016; 11(6)

Dong X, Wu P, Sun X, Li W, Wan H, Yu J XL. Intra-tumour 18F-FDG uptake heterogeneity decreases the reliability on target volume definition with positron emission tomography/computed tomography imaging. J Med Imaging Radiat Oncol 2015; 59(3):338–345

Eary JF, O'Sullivan F, O'Sullivan J, Conrad EU. Spatial Heterogeneity in Sarcoma ^{18}F-FDG Uptake as a Predictor of Patient Outcome. J Nucl Med 2008; 49(12):1973–1979

Eiber M, Maurer T, Souvatzoglou M, et al. Evaluation of hybrid ^{68}Ga-PSMA ligand PET/CT in 248 patients with biochemical recurrence after radical prostatectomy. J Nucl Med 2015; 56:668–674

Eiber M, Weirich G, Holzapfel K, et al. Simultaneous Ga-PSMA HBED-CC PET/MRI improves the localization of primary prostate cancer. Eur Urol 2016; 70(5):829-836

El Naqa I, Grigsby P, Apte A, Kidd E, Donnelly E, Khullar D, et al. Exploring feature-based approaches in PET images for predicting cancer treatment outcomes. Pattern Recognit 2009; 42:1162–1171

Fendler WP, Eiber M, Beheshti M, Bomanji J, Ceci F, Cho S, Giesel F, Haberkorn U, Hope TA, Kopka K, Krause BJ, Mottaghy FM, Schöder H, Sunderland J, Wan S, Wester HJ, Fanti S, Herrmann K. ^{68}Ga-PSMA PET/CT: Joint EANM and SNMMI procedure guideline for prostate cancer imaging: version 1.0. Eur J Nucl Med Mol Imaging. 2017; 44(6):1014-1024

Ferdinandus J, Eppard E, Gaertner FC, Kürpig S, Fimmers R, Yordanova A, et al. Predictors of Response to Radioligand Therapy of Metastatic Castrate-Resistant Prostate Cancer with 177 Lu-PSMA-617. J Nucl Med 2017; 58(2):312–319

Fidler IJ, Hart IR. Biological diversity in metastatic neoplasms: origins and implications. Science. 1982; 217:998–1003

Gahramanov S, Varallyay C, Tyson RM, et al. Diagnosis of pseudoprogression using MRI perfusion in patients with glioblastoma multiforme may predict improved survival. CNS Oncol 2014; 3:389–400

Gallamini A, Zwarthoed C, Borra A. Positron Emission Tomography (PET) in Oncology. Cancers (Basel). 2014; 6(4):1821-89

Galldiks N, Dunkl V, Stoffels G, Hutterer M, Rapp M, Sabel M*, et al.* Diagnosis of pseudoprogression in patients with glioblastoma using O-(2-[18F]fluoroethyl)-L-tyrosine PET. European journal of nuclear medicine and molecular imaging. 2015; 42(5):685-695

Galldiks N, Dunkl V, Stoffels G, Hutterer M, Rapp M, Sabel M, Reifenberger G, Kebir S, Dorn F, Blau T, Herrlinger U, Hau P, Ruge MI, Kocher M, Goldbrunner R, Fink GR, Drzezga A, Schmidt M, Langen KJ. Diagnosis of pseudoprogression in patients with glioblastoma using O-(2-[18F]fluoroethyl)-L-tyrosine PET. Eur J Nucl Med Mol Imaging. 2015 Apr; 42(5):685-695

Ganeshan B, Miles KA, Young RC, Chatwin CR. Hepatic entropy and uniformity: additional parameters that can potentially increase the effectiveness of contrast enhancement during abdominal CT. Clin Radiol 2007; 62(8):761–768

Gatenby RA, Gillies RJ. A microenvironmental model of carcinogenesis. Nat Rev Cancer. 2008; 8(1):56–61

Gatenby RA, Grove O, Gillies RJ. Quantitative imaging in cancer evolution and ecology. Radiology. 2013 Oct; 269(1):8-15

Gevaert O, Mitchell LA, Achrol AS, Xu J, Echegaray S, Steinberg GK, et al. Glioblastoma multiforme: exploratory radiogenomic analysis by using quantitative image features. Radiology. 2014; 273:168–174

Gerlinger M, Rowan AJ, Horswell S, et al. Intratumor heterogeneity and branched evolution revealed by multiregion sequencing. N Engl J Med 2012; 366:883–892

Gerlinger M. & Swanton C. How Darwinian models inform therapeutic failure initiated by clonal heterogeneity in cancer medicine. Br. J. Cancer. 2010; 103, 1139–1143

Galavis PE, Hollensen C, Jallow N, Paliwal B, Jeraj R. Variability of textural features in FDG PET images due to different acquisition modes and reconstruction parameters. Acta Oncol 2010; 49:1012–1016

Goh V, Sanghera B, Wellsted DM, Sundin J, Halligan S. Assessment of the spatial pattern of colorectal tumour perfusion estimated at perfusion CT using two-dimensional fractal analysis. Eur Radiol 2009; 19(6):1358–1365

Greaves M, Maley CC. Clonal evolution in cancer. Nature. 2012; 481(7381):306–313.

Hanahan D, Weinberg RA. Hallmarks of cancer: the next generation.Cell. 2011;144(5):646-74

Hanley J, McNeil B. The meaning and use of the area under a receiver operating characteristic (ROC) curve. Radiology. 1982;143(1):29–36

Hatt M, Tixier F, Cheze Le Rest C, Pradier O, Visvikis D. Robustness of intratumour (18)F-FDG PET uptake heterogeneity quantification for therapy response prediction in oesophageal carcinoma. Eur J Nucl Med Mol Imaging 2013; 40:1662–1671

Heppner GH. Tumor heterogeneity. Cancer Res 1984; 44:2259–2265

Hockel M, Knoop C, Schlenger K, et al. Intratumoral pO2 predicts survival in advanced cancer of the uterine cervix. Radiother Oncol 1993; 26(1):45–50

Hockel M, Schlenger K, Aral B, Mitze M, Schaffer U, Vaupel P. Association between tumor hypoxia and malignant progression in advanced cancer of the uterine cervix. Cancer Res 1996; 56(19):4509–4515

Hoffman WF, Levin VA, Wilson CB. Evaluation of malignant glioma patients during the postirradiation period. J Neurosurg 1979; 50:624–628

Horoszewicz JS, Kawinski E, Murphy GP. Monoclonal antibodies to a new antigenic marker in epithelial cells and serum of prostatic cancer patients. Anticancer Res 1987; 7:927–936

Hyun SH, Kim HS, Choi SH, Choi DW, Lee JK, Lee KH*, et al.* Intratumoral heterogeneity of F-FDG uptake predicts survival in patients with pancreatic ductal adenocarcinoma. Eur J Nucl Med Mol Imaging 2016; 43(8):1461-1468

Jemal A, Siegel R, Xu J, Ward E. Cancer statistics, 2010. CA Cancer J Clin 2010; 60:277–300

Kebir S, Fimmers R, Galldiks N, Schafer N, Mack F, Schaub C*, et al.* Late Pseudoprogression in Glioblastoma: Diagnostic Value of Dynamic O-(2-[18F]fluoroethyl)-L-Tyrosine PET. Clin Cancer Res 2016; 22(9):2190-2196

Kern, S. E. Why your new cancer biomarker may never work: recurrent patterns and remarkable diversity in biomarker failures. Cancer Res 2012; 72, 6097–6101

Khan MN, Sharma AM, Pitz M, Loewen SK, Quon H, Poulin A, Essig M. High-grade glioma management and response assessment-recent advances and current challenges. Curr Onco 2016; 23(4):383-391

Kratochwil C, Giesel FL, Stefanova M, et al. PSMA-targeted radionuclide therapy of metastatic castration-resistant prostate cancer with Lu-177 labeled PSMA-617. J Nucl Med 2016; 57:1170–1176

Kulkarni HR, Singh A, Schuchardt C, Niepsch K, Sayeg M, Leshch Y, et al. PSMA-Based Radioligand Therapy for Metastatic Castration-Resistant Prostate Cancer: The Bad Berka Experience Since 2013. J Nucl Med 2016; 57:97S–104S.

Lapa C, Werner RA, Schmid JS, Papp L, Zsótér N, Biko J, Reiners C, Herrmann K, Buck AK, Bundschuh RA. Prognostic value of positron emission tomography-assessed tumor heterogeneity in patients with thyroid cancer undergoing treatment with radiopeptide therapy. Nucl Med Biol 2015; 42(4):349-354

Liu Y, Xu X, Yin L, Zhang X, Li L, Lu H. Relationship between Glioblastoma Heterogeneity and Survival Time: An MR Imaging Texture Analysis. American Journal of Neuroradiology. 2017, 38 (9) 695-1709

Louis DN, Ohgaki H, Wiestler OD, et al. The 2007 WHO classification of tumours of the central nervous system. Acta Neuropathol 2007; 114:97–109

Lozano R, Naghavi M, Foreman K, Lim S, Shibuya K, Aboyans V, et al. Global and regional mortality from 235 causes of death for 20 age groups in 1990 and 2010: A systematic analysis for the Global Burden of Disease Study 2010. Lancet. 2012; 380(9859):2095–2128

Mathieu C, Ferrer L, Rousseau C et al.,. Assessment of Lymph Nodes and Prostate Status Using Early Dynamic Curves with ^{18}F-Choline PET/CT in Prostate Cancer. Front Med 2015; 2:67

Melguizo-Gavilanes I, Bruner JM, Guha-Thakurta N, Hess KR, Puduvalli VK. Characterization of pseudoprogression in patients with glioblastoma: is histology the gold standard? J Neurooncol 2015;123:141–150

Mikeska T, Bock C, El-Maarri O, Hubner A, Ehrentraut D, Schramm J, et al. Optimization of quantitative MGMT promoter methylation analysis using pyrosequencing and combined bisulfite restriction analysis. The Journal of molecular diagnostics 2007; 9:368-381

Molina D, Pérez-Beteta J, Luque B[1], Arregui E, Calvo M, Borrás JM, López C, Martino J, Velasquez C, Asenjo B, Benavides M, Herruzo I, Martínez-González A, Pérez-Romasanta L, Arana E, Pérez-García VM. Tumour heterogeneity in glioblastoma assessed by MRI texture analysis: a potential marker of survival. Br J Radiol 2016; 20160242

Morita K, Takeshita T, Miwa K, Maebatake A,Tsutsui Y, Himuro K, Baba S, Sasaki M. Different image reconstruction methods resulted in different level of heterogeneity in texture analysis of PET images. J Nucl Med 2016; 18: 124-29

Nicolson GL. Generation of phenotypic diversity and progression in metastatic tumor cells. Cancer Metastasis Rev 1984; 3:25–42

Nowell PC. The clonal evolution of tumor cell populations. Science1976; 194(4260):23–28

O'Sullivan F, Roy S, Eary J. A statistical measure of tissue heterogeneity with application to 3D PET sarcoma data. Biostatistics. 2003; 4:433–448

Pyka T, Bundschuh RA, Andratschke N, Mayer B, Specht HM, Papp L, et al. Textural features in pre-treatment [F18]-FDG-PET/CT are correlated with risk of local recurrence and disease-specific survival in early stage NSCLC patients receiving primary stereotactic radiation therapy. Radiat Oncol 2015; 10(1):100

Pyka T, Gempt J, Hiob D, Ringel F, Schlegel J, Bette S*, et al.* Textural analysis of pre-therapeutic [18F]-FET-PET and its correlation with tumor grade and patient survival in high-grade gliomas. European journal of nuclear medicine and molecular imaging. 2016; 43(1):133-141

Rachinger W, Goetz C, Pöpperl G, Gildehaus FJ, Kreth FW, Holtmannspötter M, Herms J, Koch W, Tatsch K, Tonn JC. Positron emission tomography with O-(2-[18F]fluoroethyl)-l-tyrosine versus magnetic resonance imaging in the diagnosis of recurrent gliomas. Neurosurgery. 2005 Sep; 57(3):505-511

Rahbar K, Ahmadzadehfar H, Kratochwil C, Haberkorn U, Schäfers M EM, Baum RP, Kulkarni HR, Schmidt M, Drzezga A, Bartenstein P, Pfestroff A LM, Lützen U, Marx M, Prasad V, Brenner W, Heinzel A, Mottaghy FM, Ruf J MP, Heuschkel M, Eveslage M, Bögemann M, Fendler WP KB. German Multicenter Study Investigating ^{177}Lu-PSMA-617 Radioligand Therapy in Advanced Prostate Cancer Patients. J Nucl Med 2017; 58(1):85–90

Rahbar K, Bode A, Weckesser M, et al. Radioligand therapy with 177Lu-PSMA617 as a novel therapeutic option in patients with metastatic castration resistant prostate cancer. Clin Nucl Med 2016; 41:522–528

Rahbar K, Schmidt M, Heinzel A, et al. Response and tolerability of a single dose of ^{177}Lu-PSMA-617 in patients with metastatic castration-resistant prostate cancer: a multicenter retrospective analysis. J Nucl Med 2016;57:1334–1338

Rahbar K, Weckesser M, Huss S, et al. Correlation of intraprostatic tumor extent with ^{68}Ga-PSMA distribution in patients with prostate cancer. J Nucl Med 2016; 57:563–567

Ross JS, Sheehan CE, Fisher HAG, et al. Correlation of primary tumor prostate-specific membrane antigen expression with disease recurrence in prostate cancer. Clin Cancer Res 2003; 9:6357–6362

Sanghera B, Banerjee D, Khan A, et al. Reproducibility of 2D and 3D Fractal Analysis Techniques for the Assessment of Spatial Heterogeneity of Regional Blood Flow in Rectal Cancer. Radiology. 2012; 263(3):865–873

Segal E, Sirlin CB, Ooi C, Adler AS, Gollub J, Chen X, et al. Decoding global gene expression programs in liver cancer by noninvasive imaging. Nat Biotechnol. 2007; 25:675–680

Silver DA, Pellicer I, Fair WR, et al. Prostatespecific membrane antigen expression in normal and malignant human tissues. Clin Cancer Res 1997; 3:81–85

Skvortsova TY, Brodskaya ZL, Gurchin AF. PET using ^{11}C–methionine in recognition of pseudoprogression in cerebral glioma after combined treatment [Russian] Zh Vopr Neirokhir Im N N Burdenko. 2014; 78:50–58

Soussan M, Orlhac F, Boubaya M, Zelek L, Ziol M, Eder V, Buvat I Relationship between tumor heterogeneity measured on FDG-PET/CT and pathological prognostic factors in invasive breast cancer. PLoS One. 2014; 9(4):e94017

Srinivasan GN, Shobha G. Statistical texture analysis. Proceedings of World Academy of Science, Engineering and Technology. 2008; 36:1264–1269

Taal W, Brandsma D, de Bruin HG, et al. Incidence of early pseudo-progression in a cohort of malignant glioma patients treated with chemoirradiation with temozolomide. Cancer. 2008; 113:405–410

Tixier F, Groves AM, Goh V, Hatt M, Ingrand P, Le Rest CC, et al. Correlation of intra-tumor 18F-FDG uptake heterogeneity indices with perfusion CT derived parameters in colorectal cancer. PLoS One. 2014; 9:e99567

Tixier F, Hatt M, Rest CCL, Simon B, Key S, Corcos L, et al. Signaling pathways alteration involved in head and neck cancer can be identified through textural features analysis in 18F-FDG PET images: a prospective study. J Nucl Med 2015; 56:449

Tixier F, Le Rest CC, Hatt M, Albarghach N, Pradier O, Metges JP, et al. Intratumor heterogeneity characterized by textural features on baseline 18F-FDG PET images predicts response to concomitant radiochemotherapy in esophageal cancer. J Nucl Med 2011; 52:369–378

Troyer JK, Beckett ML, Wright GL., Jr. Detection and characterization of the prostate-specific membrane antigen (PSMA) in tissue extracts and body fluids. Int J Cancer. 1995; 62:552–558

Tuceryan M, Jain AK. Texture analysis. The Handbook of Pattern Recognition and Computer Vision. 1998; pp. 207–248

Vincent TL, Brown JS. Evolutionary game theory, natural selection and Darwinian dynamics. Cambridge, England: Cambridge University Press, 2005

Visvikis D, Hatt M, Tixier F, Rest CLC. The age of reason for FDG PET image-derived indices. Eur J Nucl Med Mol Imaging. 2012; 39:1670–1672

Wan T, Bloch BN, Plecha D, Thompson CL, Gilmore H, Jaffe C, et al. A radio-genomics approach for identifying high risk estrogen receptor-positive breast cancers on DCE-MRI: preliminary results in predicting OncotypeDX risk scores. Sci Rep 2016; 6:21394

Weber WA, Schwaiger M, Avril N. Quantitative assessment of tumor metabolism using FDG-PET imaging. Nucl Med Biol 2000; 27:683–687

Wen PY, Macdonald DR, Reardon DA, et al. Updated response assessment criteria for high-grade gliomas: Response Assessment in Neuro-Oncology working group. J Clin Oncol 2010; 28:1963–1972

West J, Newton PK. Chemotherapeutic Dose Scheduling Based on Tumor Growth Rates Provides a Case for Low-Dose Metronomic High-Entropy Therapies. Cancer Res 2017 Dec 1; 77(23): 6717–6728

Wilkerson MD, Hayes DN. Consensus Cluster Plus: a class discovery tool with confidence assessments and item tracking. Bioinformatics. 2010;26:1572-1573

Willaime JM, Turkheimer FE, Kenny LM, Aboagye EO. Quantification of intra-tumour cell proliferation heterogeneity using imaging descriptors of ^{18}F fluorothymidine-positron emission tomography. Phys Med Biol 2013; 58:187–203

Win T, Miles KA, Janes SM, Ganeshan B, Shastry M, Endozo R, et al. Tumor heterogeneity and permeability as measured on the CT component of PET/CT predict survival in patients with non-small cell lung cancer. Clin Cancer Res 2013; 19:3591–3599

Yachida, S. et al. Distant metastasis occurs late during the genetic evolution of pancreatic cancer. Nature. 2010; 467, 1114–1117

Yan J, Chu-Shern JL, Loi HY, Khor LK, Sinha AK, Quek ST, Tham IW, Townsend D. Impact of Image Reconstruction Settings on Texture Features in 18F-FDG PET. J Nucl Med. 2015 Nov; 56(11):1667-1673

Yang Z, Tang LH, Klimstra DS. Effect of tumor heterogeneity on the assessment of Ki67 labeling index in well-differentiated neuroendocrine tumors metastatic to the liver: implications for prognostic stratification. Am J Surg Pathol 2011; 35(6):853–860

Yoon SH, Park CM, Park SJ, Yoon J-H, Hahn S, Goo JM. Tumor heterogeneity in lung cancer: assessment with dynamic contrast-enhanced MR imaging. Radiology. 2016; 280(3):940-8

Youden WJ. Index for rating diagnostic tests. Cancer. 1950;3(1):32–5

Zaidi H, Abdoli M, Fuentes CL, El Naqa IM. Comparative methods for PET image segmentation in pharyngolaryngeal squamous cell carcinoma. Eur J Nucl Med Mol Imaging 2012; 39:881–91

Zechmann CM, Afshar-Oromieh A, Armor T, Stubbs JB, Mier W, Hadaschik B, et al. Radiation dosimetry and first therapy results with a 124I/ 131I-labeled small molecule (MIP-1095) targeting PSMA for prostate cancer therapy. Eur J Nucl Med Mol Imaging. 2014; 41(7):1280–92

Zeng H, Yu H, Lu L, Jain D, Kidd MS, Saif MW, Chanock SJ, Hartge P; PanScan Consortium, Risch HA. Genetic effects and modifiers of radiotherapy and chemotherapy on survival in pancreatic cancer. Pancreas. 2011 Jul; 40(5):657-63